

This dissertation has been
microfilmed exactly as received

66-10,341

FOSTER, Peter David, 1941-
STUDIES IN MICROWAVE SPECTROSCOPY:
 ^{14}N ^{16}O ^{17}O , METHYL VINYL KETONE, AND
A SPECTROMETER FOR UNSTABLE MOLE-
CULES.

Rice University, Ph.D., 1966
Chemistry, physical

University Microfilms, Inc., Ann Arbor, Michigan

RICE UNIVERSITY

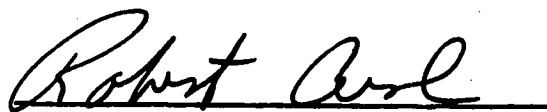
STUDIES IN MICROWAVE SPECTROSCOPY:
 $^{14}\text{N}^{16}\text{O}^{17}\text{O}$, METHYL VINYL KETONE, AND
A SPECTROMETER FOR UNSTABLE MOLECULES

by.

Peter D. ^{Gold}Foster

A THESIS SUBMITTED
IN PARTIAL FULFILLMENT OF THE
REQUIREMENTS FOR THE DEGREE OF
DOCTOR OF PHILOSOPHY

Thesis Director's signature:

A handwritten signature in cursive script, appearing to read "Robert A. Cool", is written over a horizontal line.

Houston, Texas

June, 1966

Peter D. Fortin

ABSTRACT

Some 150 hyperfine transitions belonging to the $8_{08-7}17$ and $9_{19-10}0,10$ rotational transitions of $^{14}_N^{16}_O^{17}_O$ have been observed in the microwave region. The new coupling constants which have been determined are the odd-electron expectation values on oxygen. They are

$$|\Psi(0)|^2 = 0.71 \times 10^{24} \text{ cm}^{-3},$$

$$\left\langle \frac{3\hat{f}_a^2 - 1}{r^3} \right\rangle = -4.71 \times 10^{24} \text{ cm}^{-3},$$

and $\left\langle \frac{(\hat{f}_b - i\hat{f}_c)^2}{r^3} \right\rangle = 5.04 \times 10^{24} \text{ cm}^{-3}.$

The conformation and barrier to internal rotation in methyl vinyl ketone have been determined. The most stable configuration is with the double bonds *trans* to each other, and $V_3 = 1250 \text{ cal/mole}.$

A new fast-flow, high-frequency video microwave spectrometer has been constructed to search for new unstable molecules. As yet no new chemical species have been identified.

ACKNOWLEDGEMENT

My sincere thanks to Dr. R. F. Curl for his continuing guidance during the past three years.

The generous support of a National Defense Education Act Fellowship during my entire graduate career is gratefully acknowledged.

The last two sections of Chapter I have appeared, in essence, as a publication co-authored with Drs. V. M Rao and R. F. Curl, Jr.

To my wife Judy, I shall always be grateful.

TABLE OF CONTENTS

	INTRODUCTION	1
Chapter I.	MICROWAVE SPECTRUM OF METHYL VINYL KETONE	3
	Internal Rotation	3
	Conformation	5
	Spectrum and Interpretation	6
	Discussion	12
Chapter II.	MICROWAVE SPECTRUM OF $^{14}\text{N}^{16}\text{O}^{17}\text{O}$	13
	Background	13
	Theory	16
	Experimental	32
	Spectrum and Interpretation	33
	Discussion of the Magnetic Coupling Constants	48
Chapter III.	A MICROWAVE SPECTROMETER FOR SIMPLE UNSTABLE MOLECULES	51
	Purpose	51
	Basic Design Requirements	52
	Fundamentals of Construction	55
	Prospective Molecules	58
Appendix I.	Nucleus 2 Matrix Elements Diagonal in $\text{N}\tau$	60
Appendix II.	H_{sr} and $\text{H}_{\text{dd}}(1)$ Matrix Elements Off-Diagonal in $\text{N}\tau$	62
Appendix III.	Spectrum of $^{14}\text{N}^{16}\text{O}^{17}\text{O}$ Observed by Hodgeson	64
Appendix IV.	Diagnostic Least Square	65
Bibliography	67

INTRODUCTION

Three rather different studies in microwave spectroscopy are presented in this thesis, all utilizing the excellent resolution obtainable from quantum measurements in the microwave region.

Chapter I presents a study of the microwave spectrum of methyl vinyl ketone (3-butene-2-one), a molecule with a conjugated bond system. The barrier to internal rotation of the methyl group and the steric configuration of the heavy atom skeleton of the molecule have been determined. The results of most previous work on $C=C-C=C$ systems have indicated that the most stable configuration is with the double bonds *trans* to each other, and all atoms except for two methyl hydrogens in a plane. Because of the different nature of the conjugated system ($C=C-C=O$) in methyl vinyl ketone, it was hoped that some other steric isomer might be observed.

Chapter II presents a study of the very complex rotational hyperfine spectrum of the molecule $^{14}N^{16}O^{17}O$, a stable free radical with two nuclear spins. The purpose of the study is to determine the Fermi and dipole-dipole coupling constants of the ^{17}O nucleus with the odd electron. These constants are related to the character of the odd electron orbital in the vicinity of the oxygen nucleus. The combined results of this work and previous determinations of the dipole moment and spin-rotation

and ^{14}N Fermi, dipole-dipole and quadrupole coupling constants may be used as a severe test of any proposed wave mechanical description of chemical bonding in nitrogen dioxide.

Chapter III presents the results, to date, of the use of a new microwave spectrometer for the study of simple unstable molecules. It is hoped to gain some information about the physical properties of the intermediates in chemical reactions. A fast-flow, high-frequency, video spectrometer with a free space absorption cell has been constructed, but as yet no new chemical species have been identified.

CHAPTER I
MICROWAVE SPECTRUM OF
METHYL VINYL KETONE

INTERNAL ROTATION

The presence in a non-rigid molecule of a functional group with an axis of 3-fold or higher symmetry allows the possibility of an internal torsional motion which may be treated as a special case of rotation-vibration coupling. This type of motion is generally referred to as internal rotation. If the barrier to this motion is sufficiently low, the interaction of torsion and overall rotation in a molecule is noticed in the rotational spectrum of the molecule. In the case of a molecule with a 3-fold symmetric group the triple degeneracy of the rotational energy levels associated with a particular vibrational state is partially removed and rotational transitions appear as doublets. One component of the doublet belongs to the non-degenerate A representation and the other belongs to the doubly-degenerate E representation of the C_3 symmetry group. The spacing of these doublets is dependent on the magnitude of rotation-vibration coupling, and hence on the barrier to internal rotation.

The theoretical treatment of internal rotation has received much attention¹ and is adequate for most molecules. The model for the calculation is a rigid top rotating against a rigid frame, with the symmetry axis of the top taken as the

axis of internal rotation. The origin of potential barriers is not clearly understood. The only requirement that can be placed on the potential function hindering internal rotation is that it be periodic in the relative angle α between the two parts of the molecule. In the case of a 3-fold barrier the hindering potential $V(\alpha)$ can be expressed as a cosine series expansion in 3α , such as

$$V(\alpha) = \frac{V_3}{2}(1 - \cos 3\alpha) + \frac{V_6}{2}(1 - \cos 6\alpha) + \dots \quad (1)$$

It is customary² to take the potential function simply as

$$V(\alpha) = \frac{V_3}{2}(1 - \cos 3\alpha) \quad .$$

The Hamiltonian for this system may be written as³

$$H = \frac{\hbar^2}{2} \sum_g P_g^2 / I_g + \frac{\hbar^2}{2} (p - \bar{p})^2 / r I_\alpha + V(\alpha) \quad (2)$$

where $\bar{p} = \sum_g P_g \lambda_{g\alpha} I_{g\alpha} / I_g$

g = x, y, z refers to principal axes of inertia fixed in the framework part.

P_g = components of the total angular momentum along the principal axis.

p = angular momentum of the internal top along its symmetry axis.

I_g = principal moments of inertia of the entire molecule.

I_α = moment of inertia of the top about its symmetry axis.

λ_g = direction cosines of the top axis.

$r I_\alpha$ = reduced moment of inertia of the top, where

$$r = 1 - \sum_g \lambda_{g\alpha}^2 I_g / I_g$$

The terms

$$p^2 M^2 / 2rI\alpha + V_3 / 2(1 - \cos 3\alpha) \quad (3)$$

lead to Mathieu's equation. The boundary conditions of invariance under $\alpha \rightarrow \alpha + 2\pi$ is satisfied by solutions periodic in $2\pi/3$ (A species) and those periodic in 2π (E species).

Herschbach's³ treatment of the high barrier case is applicable to methyl vinyl ketone. Briefly, the basis for a matrix representation is taken to be the Mathieu eigenfunction of (3) times the usual symmetric rotor eigenfunctions. A perturbation expansion in P is performed. Since P^2 is quadratic in the P_g , the second order terms may be combined with the rigid rotor terms from the asymmetric rotor part of the Hamiltonian. In the case of methyl vinyl ketone both the A and E series lines fit rigid rotor spectra. Higher order terms in the expansion are negligible.

Barriers to internal rotation of methyl groups in numerous molecules have been determined¹. Attempts to correlate and predict methyl barriers have generally failed⁴. However, methyl vinyl ketone belongs to a series of substituted acetone molecules in which the barrier to internal rotation is insensitive to the substituent group. The parent molecule, acetone itself, does not conform to the series.

CONFORMATION

It is not practical to undertake a complete structural determination of a molecule as complex as methyl vinyl ketone

by microwave methods. However, the steric configuration of the heavy atom skeleton of the molecule is readily determined by making reasonable estimates of the bond lengths and angles in the various possible isomers and calculating the moments of inertia of each isomer. The rotational constants determined from the spectrum of a particular rotamer will, in nearly every case, agree with only one of the possible steric configurations.

SPECTRUM AND INTERPRETATION

Methyl vinyl ketone was obtained from Matheson Coleman & Bell, and was used without further purification. The region 7-33 Gc/sec was observed with a conventional 100 Kc/sec Stark modulation spectrometer. Frequencies were measured to ± 0.3 Mc/sec. All lines were observed at dry-ice temperature.

The spectrum appeared as widely-spaced singlet and doublet lines. Assigned lines are listed in Table I. The lines at 7219.9 and 11886.9 Mc/sec have single Stark lobes to high and were assigned as the $0_{00} \rightarrow 1_{01}$ and $0_{00} \rightarrow 1_{11}$ transitions. The line at 15769.0 Mc/sec has a fast lobe to low and a slower one to high frequency and was assigned as the $1_{10} \rightarrow 2_{11}$ transition. These three lines were sufficient to determine the location of the entire spectrum. The $1 \rightarrow 2$, $2 \rightarrow 2$ and $2 \rightarrow 3$ assignments were confirmed by their Stark effects.

TABLE I
Rotational assignment of methyl vinyl ketone.

Transition	$\nu_A(\text{obs})$ (Mc/sec)	$\nu_A(\text{calc}) - \nu_A(\text{obs})$ (Mc/sec)	$(\nu_A - \nu_E)_{\text{obs}}$ (Mc/sec)	$(\nu_A - \nu_E)_{\text{calc}}$ (Mc/sec)
$0_{00} \rightarrow 1_{01}$	7 219.9	-0.1	0.0	0.3
$0_{00} \rightarrow 1_{11}$	11 886.9	-0.1	0.0	0.1
$1_{11} \rightarrow 2_{12}$	13 110.4	0.0	0.0	0.3
$1_{01} \rightarrow 2_{02}$	14 194.1	-0.2	0.0	0.6
$1_{10} \rightarrow 2_{11}$	15 769.0	-0.2	0.9	1.0
$1_{01} \rightarrow 2_{12}$	17 777.5	-0.1	0.0	0.1
$2_{12} \rightarrow 2_{21}$	17 988.5	-0.1	0.0	0.3
$2_{12} \rightarrow 3_{03}$	17 144.4	-0.4	1.0	1.0
$2_{12} \rightarrow 3_{13}$	19 524.0	0.1	0.0	0.5
$2_{02} \rightarrow 3_{03}$	20 727.8	-0.2	0.0	0.6
$3_{03} \rightarrow 3_{12}$	10 326.6	-0.6	1.4	1.5
$4_{13} \rightarrow 4_{22}$	13 163.3	-0.2	0.0	-0.1
$4_{04} \rightarrow 4_{13}$	14 473.6	-0.2	3.0	2.8
$4_{04} \rightarrow 5_{05}$	32 617.1 ^a	-0.1		1.7
$5_{14} \rightarrow 5_{23}$	14 139.5	0.1	0.7	0.9
$5_{05} \rightarrow 5_{14}$	19 894.7	-0.4	4.4	4.2
$6_{25} \rightarrow 6_{24}$	11 554.4	0.0	4.5	4.6
$6_{15} \rightarrow 6_{24}$	16 606.4	0.2	2.5	2.6
$6_{24} \rightarrow 6_{33}$	20 891.3	0.4	-1.6	-1.7
$7_{26} \rightarrow 7_{25}$	17 611.6	0.1	6.5	6.4
$7_{16} \rightarrow 7_{25}$	20 714.9	0.6	4.4	4.6

^a The E component of this transition was not measured.

The closely-spaced doublets were due to transitions between rotational energy levels which were split by torsional vibration of the methyl group. To a good approximation, both the A series and the E series lines fit rigid-rotor assignments with $A_A > A_E$, $B_A > B_E$, and $C_A = C_E$. Components of the doublets were assigned to symmetry species A or E by using these facts.

Rotational constants were obtained by least-square fitting the A series lines to a rigid-rotor energy level pattern. Rotational constants, moments of inertia and the estimated standard deviation, S, are given in Table II.

$$S = [(\nu_{\text{obs}} - \nu_{\text{calc}})^2 / (N_{\text{obs}} - N_{\text{par}})]^{1/2}$$

where N_{par} is the number of adjustable parameters. For a molecule as heavy as methyl vinyl ketone little centrifugal distortion is expected for $J < 10$. The values of $\nu_{A_{\text{calc}}} - \nu_{A_{\text{obs}}}$ probably reflect the uncertainty in measurement. The observed moments of inertia are consistent with a structure in which the two double bonds are *trans*. Little further structural information can be derived from the moments of inertia since there are three pieces of information in the moments of inertia and twenty-four structural parameters.

The spectrum in the region $0 \rightarrow 2$ appeared with single lines without any resolution with the exception of the transition $1_{10} \rightarrow 2_{11}$. This showed that the barrier due to internal rotation is high. As no lines were assigned in the excited states, the high J lines ($J > 2$) of the ground state were studied. The splittings observed for the lines are listed in

Table I.

The treatment of internal rotation used was the same as that used by Kilb, Lin and Wilson⁵ on acetaldehyde.

TABLE II

Rotational Constants and Moments of Inertia^a of the A Lines

$$A = 8941.45 \pm .06 \text{ Mc/sec}$$

$$B = 4274.48 \pm .02$$

$$C = 2945.32 \pm .02$$

$$S = 0.29 \text{ Mc/sec}$$

$$I_a = 56.521 \text{ u} \cdot \text{\AA}^2$$

$$I_b = 118.231$$

$$I_c = 171.586$$

$$I_a + I_b - I_c = I_\alpha - \Delta = 3.166 \text{ u} \cdot \text{\AA}^2$$

^aConversion factor: $5.05377 \times 10^5 \text{ u} \cdot \text{\AA}^2 \text{ Mc/sec} (C^{12} = 12.00000)$.

The methyl group axis is oriented almost parallel to the b-axis of the molecule. This makes λ_a quite small and therefore the coefficient of P_a in \mathcal{P} is quite small. The coefficient of P_b in \mathcal{P} is small because I_α/I_b is small. As a result the \mathcal{P} perturbation expansion of Herschbach³ converges rapidly and the internal rotation splittings are small. Only the terms in

Herschbach's expansions giving rise to change in the rotational constants ($\Delta A = A_A - A_E$ and $\Delta B = B_A - B_E$) are important. Then $\Delta A = \alpha^2 F \Delta \eta$ and $\Delta B = \beta^2 F \Delta \eta$; where $F = \hbar^2 / 2rI_\alpha$, $\alpha = \lambda_a I_\alpha / I_a$, $\beta = \lambda_b I_\alpha / I_b$, and $\Delta \eta$ is the difference (A minus E) of coefficients in the P expansion. Thus the quantities $\Delta \eta$ and λ_a may be determined from ΔA and ΔB .

The observed non-zero internal-rotation splittings were least-square fit to the parameters ΔA and ΔB . The calculated internal rotation parameters are given in Table III. The splittings, $\nu_A - \nu_E$ were calculated for all lines from the relation $\nu_A - \nu_E = \frac{\partial \nu}{\partial A} \Delta A + \frac{\partial \nu}{\partial B} \Delta B$. The comparisons of $(\nu_A - \nu_E)_{\text{calc}}$ with $(\nu_A - \nu_E)_{\text{obs}}$ are given in Table I. As is often the case the uncertainty in the barrier primarily arises from the uncertainty in the assumed value of I_α .

TABLE III

Internal Rotation Parameters

$\Delta A = 0.096 \pm 0.030 \text{ Mc/sec}$	
$\Delta B = 0.349 \pm 0.006 \text{ Mc/sec}$	
$s = 35.2 \pm 0.2^a$	$V_3 = 1250 \pm 20 \text{ cal/mole}$
$\lambda_b = 0.968 \pm 0.010$	$I_\alpha = 3.164 \text{ u} \cdot \text{\AA}^2^b$
$F = 1.65 \times 10^5 \text{ Mc/sec}$	

^a $V_3 = 9/4 \text{ Fs}$

^b Assumed

$9_{19} \rightarrow 10_{0,10}$

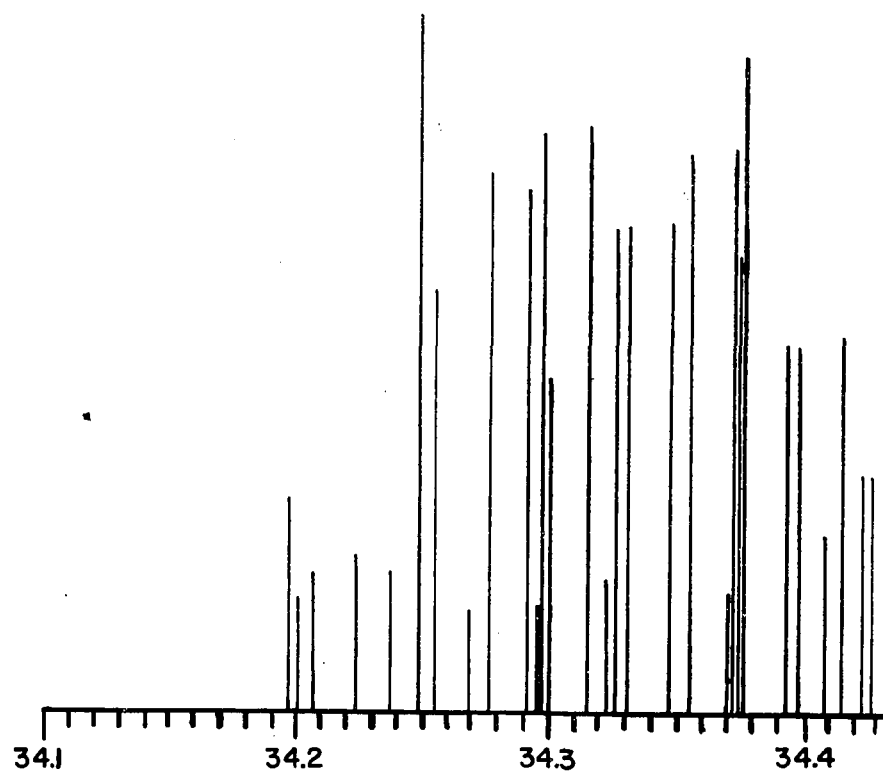
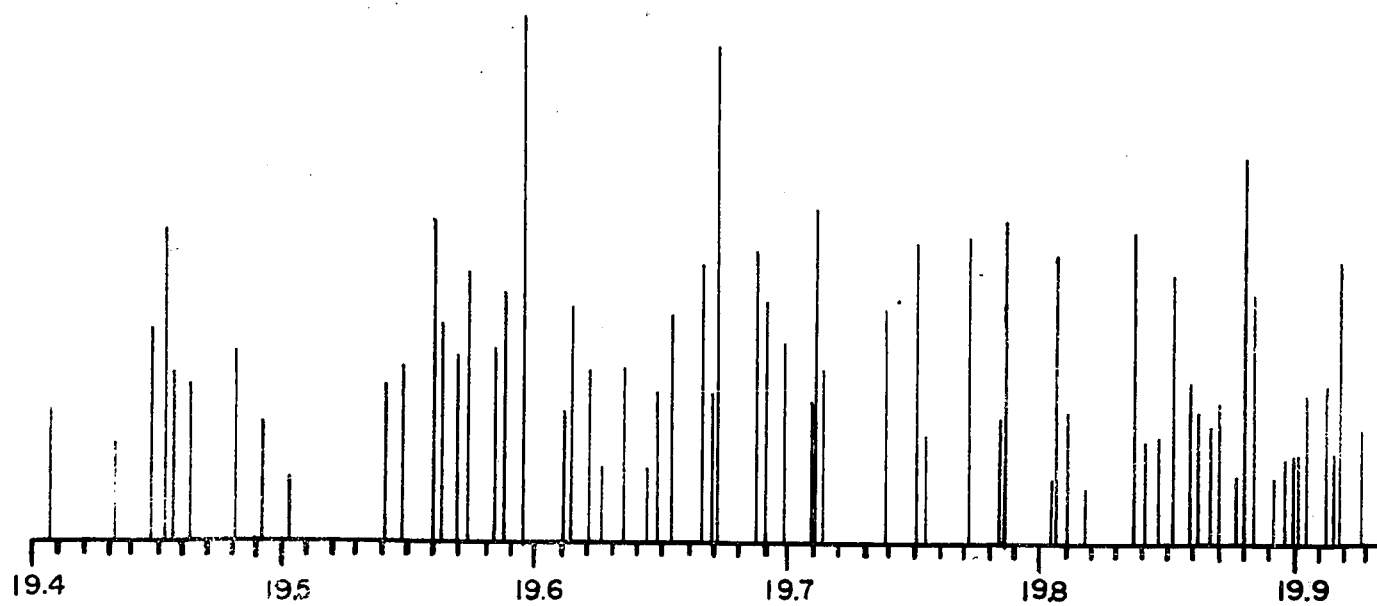


FIGURE 2

$8_{08} \rightarrow 7_{17}$



FREQUENCY

19 \rightarrow 10_{0,10}

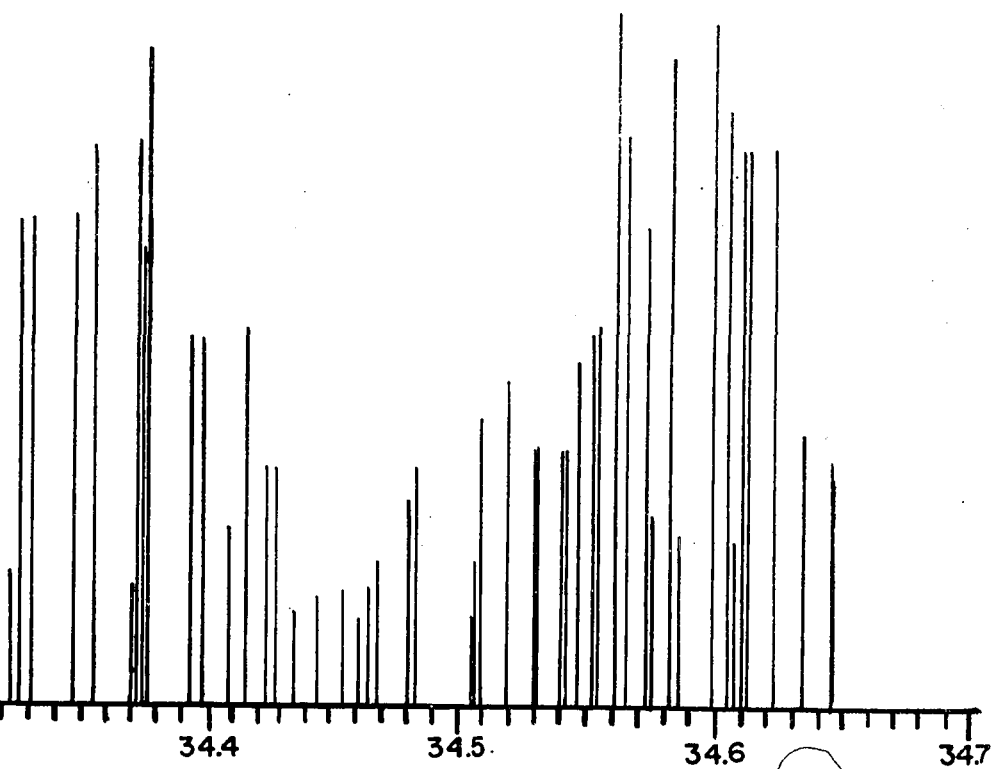
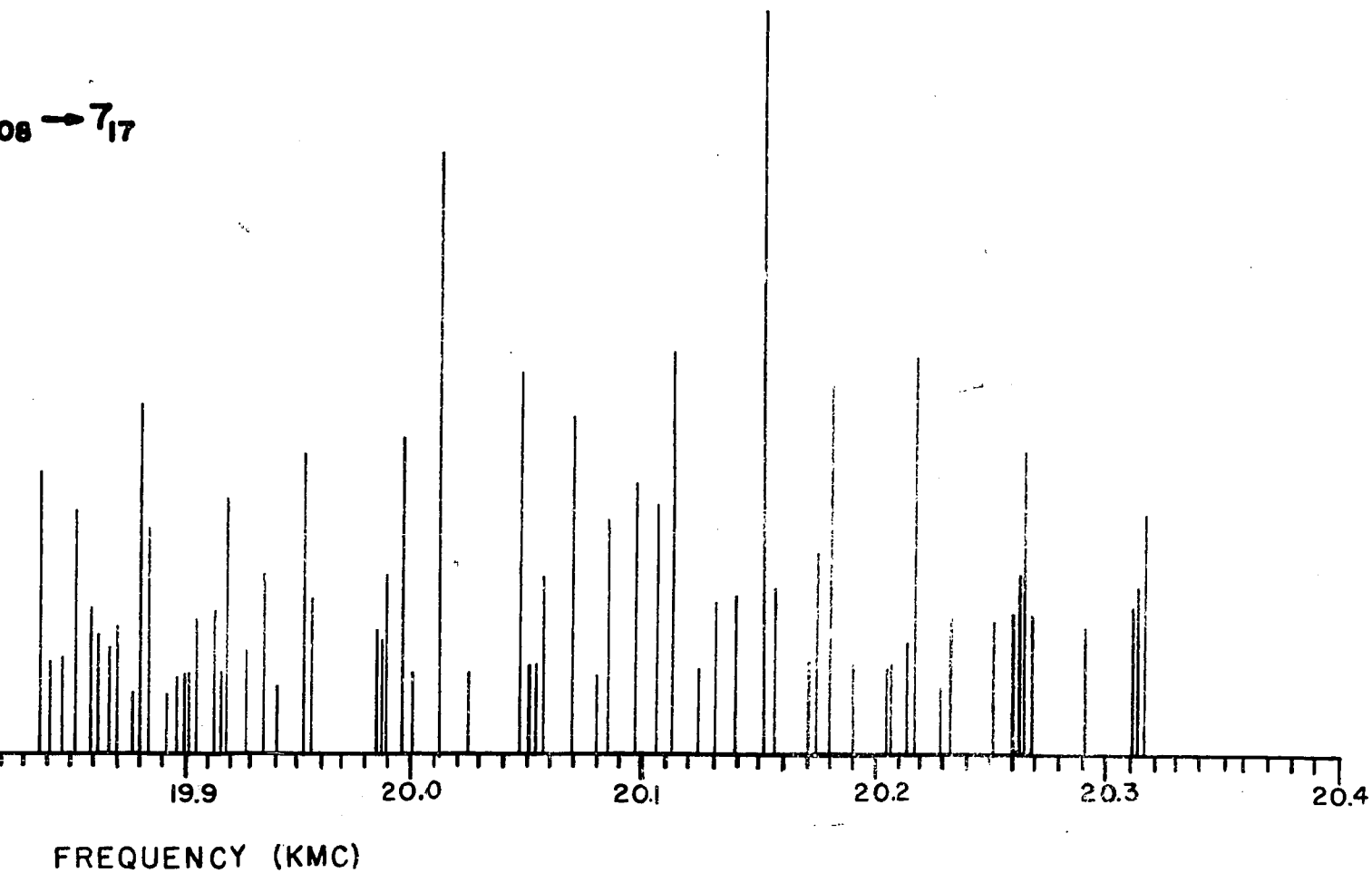


FIGURE 2

08 \rightarrow 7₁₇



The electric dipole moment was determined from Stark effect measurements on the $0_{00} \rightarrow 1_{11}$, $1_{11} \rightarrow 2_{12}$, $1_{01} \rightarrow 2_{02}$, and $1_{01} \rightarrow 2_{12}$ transitions. The components μ_a^2 and μ_b^2 were obtained by least-square fitting the observed Stark coefficients, $\frac{\Delta\nu}{E^2}$, with weighting to give a constant relative error. The observed Stark coefficients and the dipole moment are given in Table IV. Rogers⁶ gives $\mu = 2.98D$ by dielectric measurements.

DISCUSSION

This work shows that the most stable configuration of the molecule is that with the conjugated system in a *trans* configuration. No evidence was found to indicate the presence of the *cis* configuration. It would be dangerous to conclude that no other configuration exists from this negative evidence, but it would be surprising if another configuration were present in large concentrations. The structure is analagous to the results of Lide for 2-fluorobutadiene⁷ and isoprene⁸.

The barrier to internal rotation, 1250 cal/mole, is very close to that in other similar molecules¹ (CH_3CHO 1150 cal/mole, CH_3COF 1080, CH_3COC1 1350, and CH_3COCN 1270).

The discrepancy between the dielectric value and the microwave value of .18D is somewhat larger than is usually found. Often such measurements agree within 0.1D. Because of the sign ambiguities resulting on taking the square roots of μ_a^2 and μ_b^2 , there are two possible orientations of μ . One has μ directed almost along the $C \equiv O$ bond.

CHAPTER II

MICROWAVE SPECTRUM OF $^{14}\text{N}^{16}\text{O}^{17}\text{O}$

BACKGROUND

Nitrogen dioxide is a stable free radical. The study of the microwave spectrum of a free radical differs from the study of a molecule with no net electron spin. The usual pattern of energy levels associated with an asymmetric rotor is complicated by the removal of the degeneracy with respect to orientation of electron spin. In the case of $^{14}\text{N}^{16}\text{O}^{17}\text{O}$, there are also two nuclei with spin angular momenta. Coupling of the nuclear spins with the electron spin removes the degeneracy with respect to alignment of the nuclear spins. A typical rotational level is split into 36 hyperfine levels (see Figure 1). The study of $^{14}\text{N}^{16}\text{O}^{17}\text{O}$ is unique in that it is the first polyatomic molecule with an electron spin and two nuclear spins whose rotational hyperfine spectrum has been assigned.

There has been extensive work on the microwave spectrum of nitrogen dioxide⁹⁻¹⁶. Analysis of the hyperfine structure of $^{14}\text{N}^{16}\text{O}_2$, $^{15}\text{N}^{16}\text{O}_2$, and $^{14}\text{N}^{16}\text{O}^{18}\text{O}$ proceeded over a period of 15 years in several laboratories. The assignment was reported by Bird *et al.*¹⁴ in 1964. They give a detailed account of the steps leading to the assignment. The chief problems were a lack of prior knowledge of the magnitude of the hyperfine coupling constants, and the difficulty

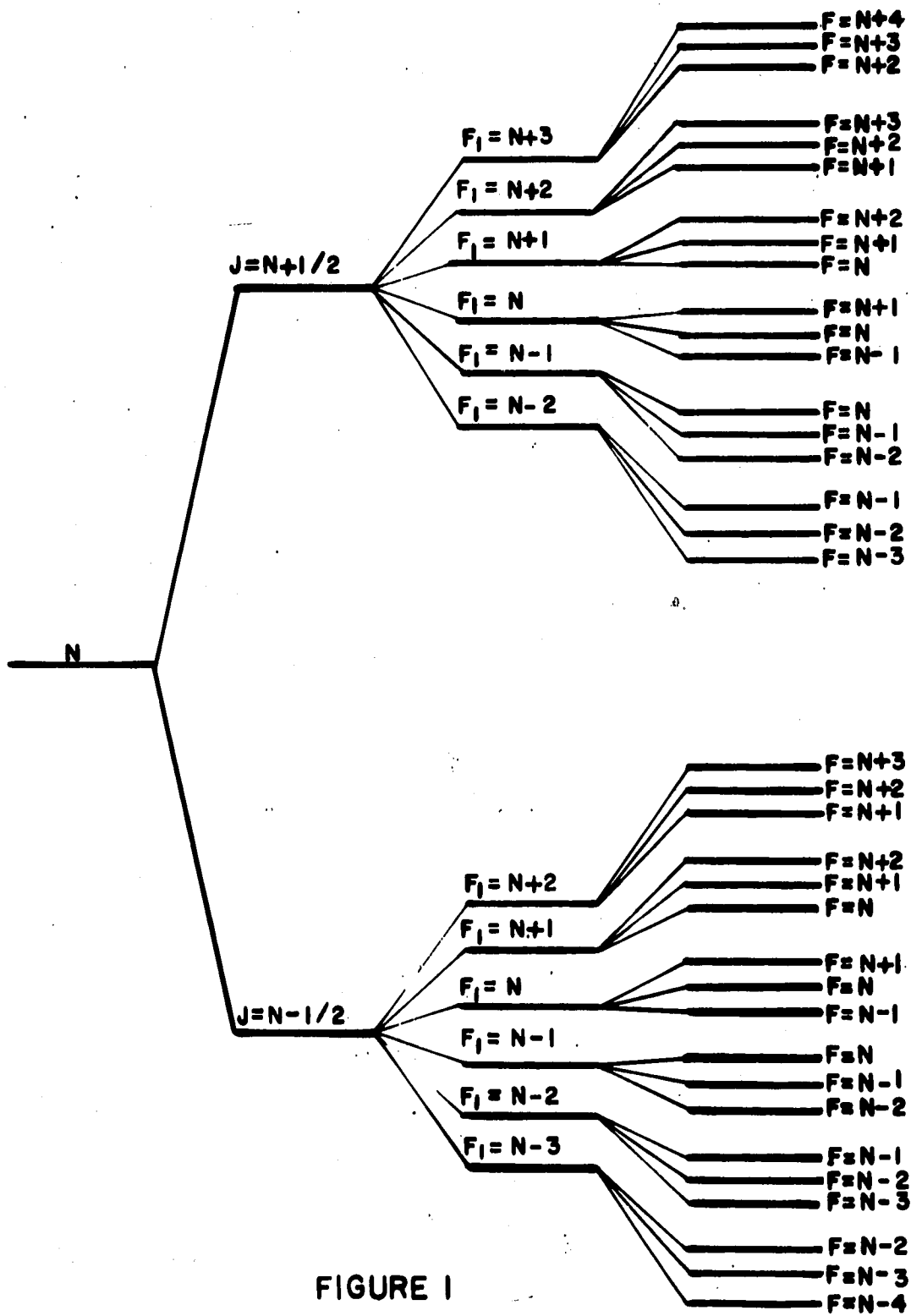


FIGURE 1

in settling on a unique mathematical solution to the problem with the limited amount of data obtainable. The dipole moment of nitrogen dioxide determined by the Stark effect of an $8_{08}-7_{17}$ transition was reported by Hodgeson, Sibert, and Curl in 1963¹⁷.

Bird *et al.*¹⁴ also discussed the magnetic coupling constants ($(0)_I$, $(aa)_I$, etc.) in terms of a simplified electronic structure. The symmetry of the odd electron orbital was determined and the percentage 2sN and 2pN character of the odd electron was estimated.

The study of $^{14}\text{N}^{16}\text{O}^{17}\text{O}$ was undertaken primarily to obtain similar information about the behavior of the odd electron in the vicinity of the oxygen atom. The knowledge of the dipole-dipole and Fermi coupling constants for the ^{17}O nucleus would then, when combined with the previous work by Bird *et al.*¹⁴ and Hodgeson, Sibert, and Curl¹⁷ represent a rather complete characterization of the ground electronic state of the molecule. Previous to this work, this much information on the ground electronic state of any bent triatomic molecule had not been available. The combined data on nitrogen dioxide should serve as a severe test of any complete wave-mechanical description of chemical bonding in the molecule.

The new information is not available from the study of ^{16}O or ^{18}O containing isotopes since they have no nuclear spin.

The microwave spectrum of $^{14}\text{N}^{16}\text{O}^{17}\text{O}$ was first observed by Hodgeson¹⁶. The lines he measured are given in Appendix III. In addition, he developed most of the computational methods necessary to analyze a rotating asymmetric molecule with an electron spin and two nuclear spins. There was also available to this author an unpublished spectrum of the $8_{08} \rightarrow 7_{17}$ region with approximate frequency markers, also obtained by Hodgeson. It is noteworthy that Dr. Hodgeson also contributed greatly to the analysis of the hyperfine spectra of $^{14}\text{N}^{16}\text{O}_2$, $^{15}\text{N}^{16}\text{O}_2$, and $^{14}\text{N}^{16}\text{O}^{18}\text{O}$. He was not able to continue the study of $^{14}\text{N}^{16}\text{O}^{17}\text{O}$ in the time available to him.

This work presents an extensive study of the regions of the $8_{08} \rightarrow 7_{17}$ and $9_{19} \rightarrow 10_{0,10}$ rotational transitions of $^{14}\text{N}^{16}\text{O}^{17}\text{O}$. The observed spectrum is shown in Figure 2. Nearly all of the observed lines have been assigned to $^{14}\text{N}^{16}\text{O}^{17}\text{O}$ and the ^{17}O magnetic coupling constants have been well determined.

THEORY

Nitrogen dioxide is one of the few chemical species whose ground electronic state exhibits a net electron spin angular momentum (S). Other molecules of this type whose hyperfine microwave spectra have been investigated are OH, SO, O_2 , NO and ClO_2 ¹⁸⁻²². The application of the tensor coupling method to the analysis of the hyperfine

$9_{19} \rightarrow 10_{0,10}$

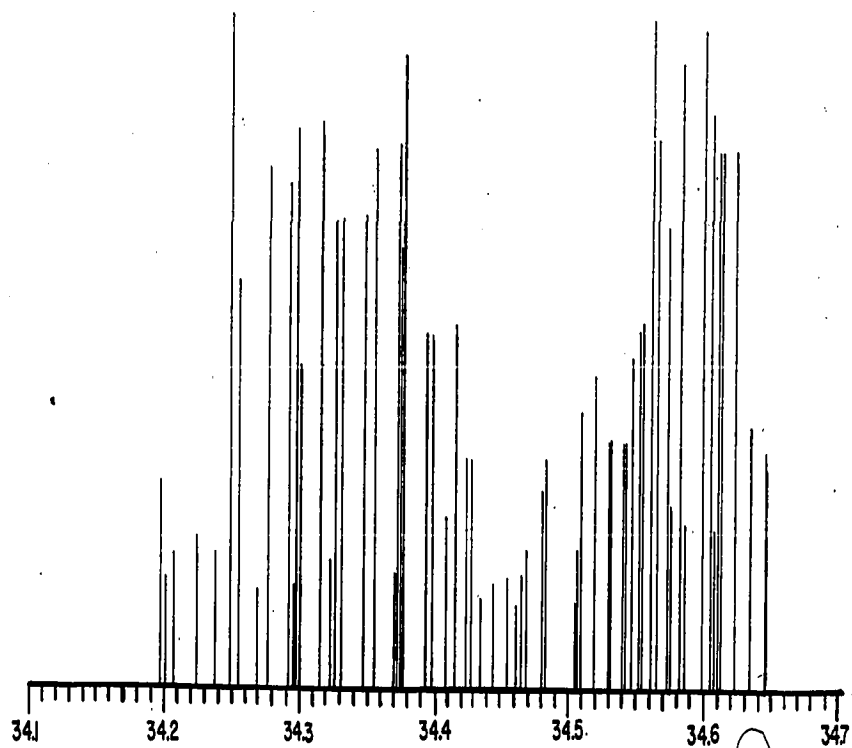
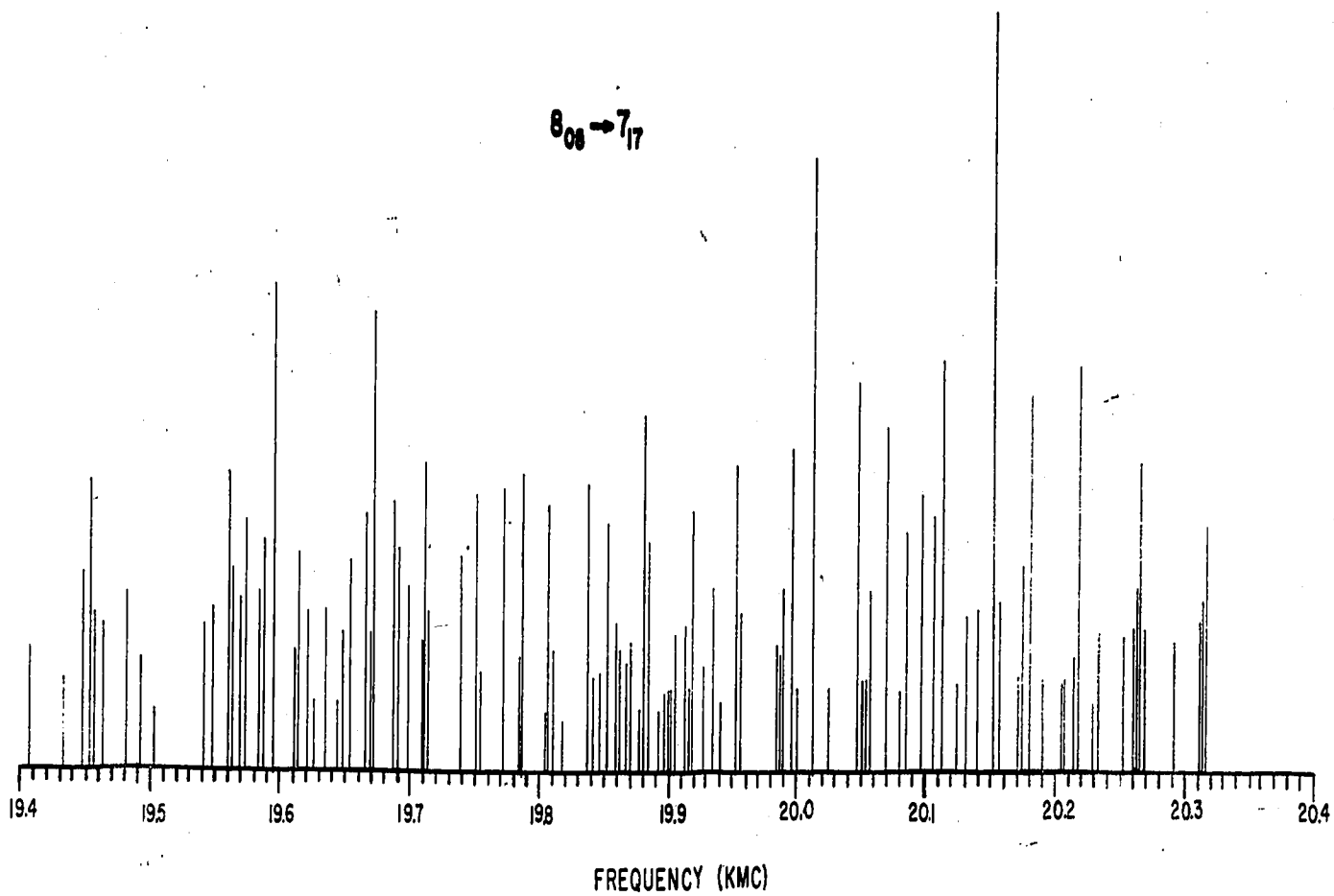


FIGURE 2

$8_{08} \rightarrow 7_{17}$



structure of free radicals was first made by Curl and co-workers on ClO_2 ²². The method is appropriate for a molecule with any degree of asymmetry. It was subsequently used in the final analysis of the spectra of the NO_2 isomers previously mentioned^{14,16}. A straightforward extension of their equations was used in calculating the new matrix elements appropriate to the $^{14}\text{N}^{16}\text{O}^{17}\text{O}$ Hamiltonian.

In the species $^{14}\text{N}^{16}\text{O}^{17}\text{O}$ there are, in addition to electron spin, nuclear spins associated with the ^{17}O ($I_1 = 5/2$) and ^{14}N ($I_2 = 1$) nuclei. In the absence of coupling between spin and mechanical angular momenta (N) the molecule would have the usual pattern of energy levels associated with an asymmetric rotor. However, the interaction of rotation with electron spin removes the $2S+1$ (two) fold degeneracy with respect to orientation of electron spin. Furthermore, the interaction of nuclear spin with electron spin and the interaction of the nuclear quadrupoles with their field environments remove the $2I_1+1$ (six) fold degeneracy with respect to alignment of the ^{17}O nuclear spin and the $2I_2+1$ (three) fold degeneracy with respect to alignment of the ^{14}N nucleus. The resulting hyperfine levels for a typical rotational energy level are indicated in Figure 1.

The calculation of the hyperfine splitting of a rotational energy level is carried out in three steps.

First, an effective Hamiltonian is derived. Next, a coupling scheme for the angular momenta is chosen. This is equivalent to choosing a set of basis functions for computing the Hamiltonian matrix. Lastly, the matrix elements are calculated and Hamiltonian matrix is diagonalized.

The Hamiltonian for a system with rotational, electronic and nuclear spin states has been discussed by several authors. Curl and Kinsey²³ have given the operators in spherical tensor notation which is appropriate for the tensor coupling method used here. The Hamiltonian has the form

$$H = H_0 + H_{sr} + H_{dd}(1) + H_f(1) + H_q(1) + H_{dd}(2) + H_f(2) + H_q(2). \quad (4)$$

H_0 is the asymmetric rotor Hamiltonian. H_{sr} is the operator describing the interaction of electron spin and mechanical rotation. $H_{dd} + H_f$ describes the interaction of the nuclear and electron magnetic dipoles. H_q is the nuclear quadrupole term. The nuclear interactions are written separately for the ^{17}O and ^{14}N nuclei.

The explicit form of the Hamiltonian is central to the solution of this problem, and it is presented here for completeness. It is discussed in detail by a number of authors²³⁻²⁵.

H_0 is the Hamiltonian of a rigid asymmetric rotor and is given by

$$H_o = AN_a^2 + BN_b^2 + CN_c^2 \quad (5)$$

where A, B, and C are the rotational constants for a rigid molecule. N_a , N_b , and N_c are the operators associated with overall rotation about the principal axes of the molecule. The eigenvalues of H_o are known²⁶.

The H_{sr} term has been derived by Van Vleck²⁷. The notation of Curl and Kinsey²³ is used here. There are significant first and second order contributions. The first order effect is the direct interaction of rotation and electron spin magnetic dipoles. The second order effect arises from two sources.

$$H_{sr(a)} = -2(AN_a L_a + BN_b L_b + CN_c L_c), \quad (6)$$

where \underline{L} is the total orbital angular momentum. This occurs because the rotational energy of the molecule is $AR_a^2 + BR_b^2 + CR_c^2$, where $\underline{R} = \underline{N} - \underline{L}$. The other second order term is

$$H_{sr(b)} = \sum n_{sj} \cdot s_j, \quad (7)$$

where n_{sj} is the spin-orbit coupling operator for electron j . The second order terms are off-diagonal in electronic energy. After a Van Vleck transformation²⁸, the ground electronic state is associated with a Hamiltonian which has the same form as the first order term. The effective spin-rotation Hamiltonian is then

$$H_{sr(eff)} = A_s N_a S_a + B_s N_b S_b + C_s N_c S_c \quad (8)$$

The interaction between electron spin and nuclear spin is the result of the two terms $H_{dd} + H_f$. There is

the classical energy of interaction between two dipoles,

$$H_{dd} = g_I g_S \mu_N \mu_B \left[\frac{\underline{S} \cdot \underline{I}}{r^3} - \frac{3(\underline{I} \cdot \underline{r})(\underline{S} \cdot \underline{r})}{r^5} \right] \quad (9)$$

where g_I is the nuclear g factor, g_S is the electron g factor, μ_N is the nuclear magneton, μ_B is the Bohr magneton, and \underline{r} is the radius vector of the electron with respect to the nucleus. The other term, H_f , may be thought of as arising as a correction to H_{dd} because the classical expression is derived assuming a finite distance between the interacting dipoles. This is not correct for the case of an electron in an s orbital. There is a non-zero probability that the electron will be at the nucleus ($\underline{r} = 0$). The correction term is called the Fermi, or contact term, and has the form

$$H_f = -8\pi/3 g_I g_S \mu_N \mu_B |\psi(0)|^2 (\underline{I} \cdot \underline{S}) \quad (10)$$

with $\mu_n > 0$ and $\mu_B > 0$.

H_q arises from the interaction of the nuclear electric quadrupole moment and the gradient of the electric field at the nucleus. It has the form

$$\frac{-eQ}{2I(2I-1)} \left[\frac{\partial^2 V}{\partial a^2} I_a^2 + \frac{\partial^2 V}{\partial b^2} I_b^2 + \frac{\partial^2 V}{\partial c^2} I_c^2 \right] \quad (11)$$

where e is the electronic charge, Q is the quadrupole moment of the nucleus, and V is the potential field at the nucleus due to electrons.

The terms H_{sr} , H_{dd} , H_f , and H_q in (4) are referred to as the hyperfine Hamiltonian. The form of the terms presented here is for a molecule with C_{2v} symmetry. For the

molecule $^{14}\text{N}^{16}\text{O}^{17}\text{O}$ the symmetry is slightly broken. The justification for this approximation is that, within experimental error, the observed hyperfine spectrum can be analyzed using (4). This was also the case in $\text{Cl}^{35}\text{O}^{16}\text{O}^{18}$ ^{22(b)}.

The coupling constants which may be determined from the spectrum of $^{14}\text{N}^{16}\text{O}^{17}\text{O}$ are listed in Table V. The notation of Curl and Kinsey²³ is used.

TABLE V

Hyperfine Coupling Constants and the Hyperfine Hamiltonian^{a,c}

$$\begin{aligned}
 H_{sr} &= A_s N_a S_a + B_s N_b S_b + C_s N_c S_c \quad b \\
 H_{dd} &= (aa)_I I_a S_a + (bb)_I I_b S_b + (cc)_I I_c S_c \\
 (aa)_I + (bb)_I + (cc)_I &= 0 \\
 (aa)_I &= -g_S g_I \mu_B \mu_N \left\langle \frac{1-3\hat{r}_a^2}{r^3} \right\rangle_{av}^d \\
 (bb)_I &= -g_S g_I \mu_B \mu_N \left\langle \frac{1-3\hat{r}_b^2}{r^3} \right\rangle_{av} \\
 (cc)_I &= -g_S g_I \mu_B \mu_N \left\langle \frac{1-3\hat{r}_c^2}{r^3} \right\rangle_{av} \\
 H_f &= (0)_I (I \cdot S) \\
 (0)_I &= -(8\pi/3) g_I g_S \mu_B \mu_N |\psi(0)|^2 ; \mu_B > 0, \mu_N > 0 \\
 H_q &= (aa)_Q I_a^2 + (bb)_Q I_b^2 + (cc)_Q I_c^2 \\
 (aa)_Q + (bb)_Q + (cc)_Q &= 0 \\
 (aa)_Q &= \frac{-eQ}{2I(2I-1)} \frac{\partial^2 V}{\partial a^2}
 \end{aligned}$$

TABLE V (continued)

Hyperfine Coupling Constants and the Hyperfine Hamiltonian^{a,c}

$$(bb)_Q = \frac{-eQ}{2I(2I-1)} \frac{\partial^2 V}{\partial b^2}$$

$$(cc)_Q = \frac{-eQ}{2I(2I-1)} \frac{\partial^2 V}{\partial c^2}$$

^aThe notation of Curl and Kinsey is used.

^bThe spin-rotation coupling constants depend on the electronic structure of the molecule, including excited states. See Reference (23).

^cThe subscript I and subscript Q parameters may be determined for ¹⁴N and ¹⁷O.

^dThe \hat{r}_a , \hat{r}_b , \hat{r}_c are unit vector components from the nucleus to odd electron.

The choice of a set of basis functions is complicated by the presence of two nuclear spins. Let us first consider a molecule such as ¹⁴N¹⁶O₂ with one nuclear spin. If the rotational, electronic, and spin wave functions are combined in a manner which makes the complete wave function an eigenfunction of the total angular momentum \underline{F} , then the Hamiltonian matrix will be block diagonal in \underline{F} (since $[\underline{H}\underline{F} - \underline{F}\underline{H}] = 0$). \underline{F} is the resultant of \underline{N} , \underline{S} and \underline{I} . There are three possible schemes for forming \underline{F} . They are:

- 1, J scheme $\underline{N} + \underline{S} = \underline{J}; \quad \underline{J} + \underline{I} = \underline{F}$
- 2, G scheme $\underline{I} + \underline{S} = \underline{G}; \quad \underline{G} + \underline{N} = \underline{F}$
- 3, E scheme $\underline{N} + \underline{I} = \underline{E}; \quad \underline{E} + \underline{S} = \underline{F}$.

The scheme to be chosen depends on which term in the Hamiltonian makes the dominant contribution to the magnitude of the hyperfine splittings. With the choice of coupling scheme is implied a prescription for writing the basis function. For the J scheme the basis is, in Dirac notation,

$$|N \tau S J I F M_F\rangle .$$

The symbols imply the eigenvectors of the set of operators N^2 , S^2 , J^2 , I^2 , F^2 , and F_z . Experimentally, it is found that the J scheme is appropriate for all the observed transitions of $^{14}\text{N}^{16}\text{O}_2$.

In $^{14}\text{N}^{16}\text{O}^{17}\text{O}$ the spin-rotation interaction is also the dominant term in the hyperfine Hamiltonian. But the presence of spin angular momentum associated with ^{17}O (which we now call I_1) leaves an ambiguity in the coupling scheme which may be described as

$$\begin{array}{ll} F_1 \text{ scheme} & \underline{N} + \underline{S} = \underline{J}; \quad \underline{J} + \underline{I}_1 = \underline{F}_1; \quad \underline{F}_1 + \underline{I}_2 = \underline{F} \\ F_2 \text{ scheme} & \underline{N} + \underline{S} = \underline{J}; \quad \underline{J} + \underline{I}_2 = \underline{F}_2; \quad \underline{F}_2 + \underline{I}_1 = \underline{F}. \end{array}$$

The choice of F_1 or F_2 coupling is nearly arbitrary since the magnitudes of the hyperfine parameters related to nucleus 1 and nucleus 2 are expected to be similar. The F_1 scheme is chosen for convenience in calculating the second order spin-rotation dipole-dipole interaction, which is found to be important for the ^{17}O nucleus. This interaction is discussed below. The basis function associated with the F_1 scheme is

$$|N \tau S J I_1 F_1 I_2 F M_F\rangle ,$$

where τ is the asymmetric rotor quantum number. The fact that there is no clear basis for choosing between the F_1 and the F_2 coupling schemes suggests that there will be strong mixing of the two schemes. It then is to be expected that transitions will occur in which $\Delta N = \Delta F \neq \Delta F_1$.

The calculation of the Hamiltonian matrix elements is carried out using the tensor coupling method. This method has been successfully applied in analyzing the hyperfine spectra of $^{35}\text{Cl}^{16}\text{O}_2$, $^{37}\text{Cl}^{16}\text{O}_2$, $^{35}\text{Cl}^{16}\text{O}^{18}\text{O}$, $^{14}\text{N}^{16}\text{O}_2$, $^{15}\text{N}^{16}\text{O}_2$, and $^{14}\text{N}^{16}\text{O}^{18}\text{O}$ ^{22,14}. Original developments in the application of the theory of tensors to the coupling of angular momenta were made by Racah²⁹ and Wigner³⁰. Edmonds³¹ has given an extended treatment of this topic. The first application of the method to the treatment of hyperfine structure in molecules is found in the works of Curl and Kinsey^{22(c), 23}. Their paper on the calculation of matrix elements of the hyperfine Hamiltonian is a primary reference for this work. A brief discussion of the method is given below.

The operators in the Hamiltonian are expressed as spherical tensor operators. Curl and Kinsey²³ have done this for all the operators of interest here, and have also given some useful relations between spherical and Cartesian tensors. The matrix elements of the hyperfine Hamiltonian

are calculated in the uncoupled scheme and the elements in the coupled scheme are obtained by the use of vector recoupling coefficients.

Any interaction term in the $^{14}\text{N}^{16}\text{O}^{17}\text{O}$ Hamiltonian can be expressed as

$$\{[\underline{T}(k_1) \times \underline{U}(k_2)]_{k_{12}} \times \underline{V}(k_3)\}_{k_{123}} \times \underline{Z}(k_4) = \underline{X}(k) \quad (12)$$

By this is meant that a tensor of rank k , $\underline{T}(k_1)$, couples with a tensor of rank k_2 , $\underline{U}(k_2)$, to give a resultant of rank k_{12} . $\underline{V}(k_3)$ then couples with

$$[\underline{T}(k_1) \times \underline{U}(k_2)]_{k_{12}}$$

to give a resultant tensor of rank k_{123} . The tensor $\underline{X}(k)$ is the resultant of coupling of $\underline{Z}(k_4)$ with the resultant of rank k_{123} .

In the F_1 coupling scheme $\underline{T}(k_1)$ is related to the operator N^2 , $\underline{U}(k_2)$ to S^2 , $\underline{V}(k_3)$ to I_1^2 , $\underline{Z}(k_4)$ to I_2^2 and $\underline{X}(k)$ to F^2 .

The equation (13) relating the matrix elements in the uncoupled scheme to those in the coupled scheme is obtained directly by another iteration of equation (2) of reference (23) using equation 7.1.5 of Edmonds' book³¹.

$$\begin{aligned} & \langle N' \tau' S J' I_1 F' I_2 F' | \underline{X}(k) | N T S J I_1 F I_2 F \rangle \\ &= [(2F+1)(2F'+1)(2k+1)(2F_1+1)(2F_1'+1) \\ & \quad (2k_{123}+1)(2J+1)(2J'+1)(2k_{12}+1)]^{1/2}. \end{aligned}$$

(continued on next page)

$$\begin{aligned}
& \left\{ \begin{matrix} F_1' & F_1 & k_{123} \\ I_2 & I_2 & k_4 \\ F' & F & k \end{matrix} \right\} \cdot \left\{ \begin{matrix} J' & J & k_{12} \\ I_1 & I_1 & k_3 \\ F_1 & F_1 & k_{123} \end{matrix} \right\} \cdot \left\{ \begin{matrix} N' & N & k_1 \\ S & S & k_2 \\ J' & J & k_{12} \end{matrix} \right\} \\
& \langle N' \tau' \| \underline{T}(k_1) \| N \tau \rangle \langle S \| \underline{U}(k_2) \| S \rangle \langle I_1 \| \underline{V}(k_3) \| I_1 \rangle \\
& \langle I_2 \| \underline{Z}(k_4) \| I_2 \rangle.
\end{aligned} \tag{13}$$

This expression was first obtained by Hodgeson¹⁶. The terms in curly brackets are Wigner 9j symbols. Edmonds³¹ has given useful relations for evaluating the 9j symbols. In particular, if any of the k's are zero the 9j reduces to the product of a 6j symbol and a simple function of elements of the 9j. The double line implies that the quantity is a reduced matrix element. They are related to the actual matrix elements by Wigner 3j symbol. For example,

$$\begin{aligned}
\langle F' \| X(k) \| F \rangle &= (-1)^{M'_F - F'} \langle F' M'_F | X(k, Q) | F M_F \rangle; \tag{14} \\
&\left(\begin{matrix} F' & k & F \\ -M'_F & Q & M_F \end{matrix} \right)^{-1}, \text{ where}
\end{aligned}$$

$X(k, Q)$ is the Q^{th} element of the rank k spherical tensor.

The Hamiltonian matrix is nearly block diagonal in the rotational quantum number N. The matrix elements off-diagonal in N can be reduced to fourth order in the energy by application of a Van Vleck perturbation²⁸. When this is done, the matrix elements associated with block N have the form (F_1 coupling scheme)

$$\begin{aligned}
& \langle NTJF | H | NTJ' F_1' F \rangle \\
& = \langle NT | H_0 | NT \rangle + \langle NTJF_1 F | H_1 | NTJ' F_1' F \rangle \\
& + \frac{1}{2} \sum_{\substack{N'' \neq N, \\ J'', F_1''}} \frac{\langle NTJF_1 F | H_1 | N'' T'' J'' F_1'' F \rangle \langle N'' T'' J'' F_1'' F | H_1 | NTJ' F_1' F \rangle}{E(NTJF_1 F) - E(N'' T'' J'' F_1'' F)} \quad (15) \\
& + \frac{\langle NTJF_1 F | H_1 | N'' T'' J'' F_1'' F \rangle \langle N'' T'' J'' F_1'' F | H_1 | NTJ' F_1' F \rangle}{E(NTJ' F_1' F) - E(N'' T'' J'' F_1'' F)},
\end{aligned}$$

where H is the total Hamiltonian, H_0 is the asymmetric rotor Hamiltonian, and H_1 is the hyperfine Hamiltonian.

The energy is expected to be correct to second order in $H_1/\Delta E$.

The first two terms in (15) are diagonal in NT . The matrix elements, diagonal in NT , associated with nucleus 1 are the same as those previously used for the work on ClO_2 ²² and NO_2 ¹⁴. Nucleus 2 matrix elements diagonal in NT were first calculated by Hodgeson¹⁶, and are given in Appendix I.

Terms in the summation are all much smaller than the first two terms in (15) because of the large energy denominator. It can be shown for the parameters obtained for $^{14}N^{16}O^{17}O$ that only a few terms in the summation over N'' , J'' , F_1'' contribute significantly to the hyperfine spectrum within the accuracy of our measurements. These "correction" matrix elements are of the type $\Delta N = \pm 1$, $\Delta K = 0$. The calculation of these matrix elements may be simplified by ignoring the slight asymmetry of the molecule and using the Wang symmetric top basis³²,

$$|NK_{-1}\gamma JF_1F\rangle, \text{ where}$$

$$|NK_{-1}\gamma\rangle = \frac{1}{\sqrt{2}}[|NK_{-1}\rangle + (-1)^\gamma |N-K_{-1}\rangle].$$

A further simplification of (15) is made by recognizing that

$$E(N\tau JF_1F) - E(N''\tau''J''F_1''F) \cong$$

$$E(N\tau J_+F_1F) - E(N''\tau''J''F_1''F) \cong E(N\tau) - E(N''\tau'') \quad (16)$$

When H_1 is written as $H_f(1) + H_{dd}(1) + H_q(1) + H_f(2) + H_{dd}(2) + H_q(2)$, with the number 1 terms related to the ^{17}O nucleus, the significant contributions to the summation in (15) are;

$$E_+ = \frac{|\langle N+1K_{-1}\gamma JF_1F | H_{sr} | NK_{-1}\gamma JF_1F \rangle|^2}{E(N\tau) - E(N+1\tau)},$$

$$E_- = \frac{|\langle NK_{-1}\gamma JF_1F | H_{sr} | N-1K_{-1}\gamma JF_1F \rangle|^2}{E(N\tau) - E(N-1\tau)},$$

$$e_+ =$$

$$\frac{2\langle NK_{-1}\gamma J_+F_1F | H_{sr} | N+1K_{-1}\gamma' J_+F_1F \rangle \langle N+1K_{-1}\gamma' J_+F_1F | H_{dd}(1) | NK_{-1}\gamma J_+F_1F \rangle}{E(N\tau) - E(N+1\tau)},$$

$$e_- = e_+ \text{ with } N \text{ replaced by } N-1 \text{ and } J_+ \text{ replaced by } J_-, \text{ and}$$

$$e_{\pm} =$$

$$\frac{\langle NK_{-1}\gamma J_+F_1F | H_{sr} | N+1K_{-1}\gamma' J_+F_1F \rangle \langle N+1K_{-1}\gamma' J_+F_1F | H_{dd}(1) | NK_{-1}\gamma J_-F_1F \rangle}{E(N\tau) - E(N+1\tau)}$$

$$+$$

$$\frac{\langle NK_{-1}\gamma J_+F_1F | H_{dd}(1) | N-1K_{-1}\gamma' J_-F_1F \rangle \langle N-1K_{-1}\gamma' J_-F_1F | H_{sr} | NK_{-1}\gamma J_-F_1F \rangle}{E(N\tau) - E(N-1\tau)}$$

where $J_+ = N+S$ and $J_- = N-S$. The matrix elements off-diagonal in N are given in Appendix II. For the molecule ClO_2 ^{22(b)} it was also necessary to include all but the e_{\pm} term in fitting the hyperfine spectrum.

TABLE VI
Magnitude of Various Contributions to the
Hyperfine Structure of the 7_{17} Level

^a

E_o	$\approx 9 \times 10^5$	Mc/sec
E_{sr}	\approx	200
$E_f(2)$	\approx	70
$E_f(1)$	\approx	35
$E_{dd}(1)$	\approx	10
E_+, E_-	\approx	10
$E_{dd}(2)$	\approx	5
$E_q(2)$	\approx	2
e_+, e_-	\approx	1
e_{\pm}	\approx	0.5
$E_q(1)$	\approx	0

^a The hyperfine quantities are intended to represent average values, and may not be correct for any particular hyperfine level.

The magnitude of the contribution from each term in (15) is indicated in Table VI for the 7_{17} rotational level, which is typical of the two rotational transitions studied here.

In the F_1 coupling scheme the hyperfine Hamiltonian matrix of dimension 36×36 associated with a rotational level N (for $N \geq 4$) factors into 9 subblocks. They are of dimension 1×1 , 3×3 , 5×5 , 6×6 , 6×6 , 6×6 , 5×5 , 3×3 , and 1×1 for F equal to $N+4$, $N+3$, $N+2$, $N+1$, N , $N-1$, $N-2$, $N-3$, and $N-4$ respectively.

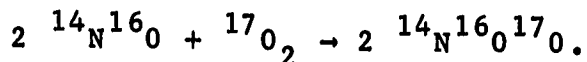
The computation of matrix elements and diagonalization of the Hamiltonian matrix were carried out on the Rice University Computer. In the assignment of intermediate quantum numbers to the calculated eigenvalues, a complication occurs in $^{14}_N^{16}O^{17}O$ which does not exist for the NO_2 isomers with only one nuclear spin. In the case of the larger subblocks of the Hamiltonian matrix it is not clear which values of the intermediate quantum numbers J and F_1 correlate with the eigenvalues obtained after diagonalization. This is equivalent to saying that the off-diagonal elements in the matrix are large enough to cause a significant mixing of coupling schemes. The intermediate angular momenta are no longer constants of the motion and the quantum numbers J and F_1 have no meaning. To distinguish eigenvalues in the same F subblock of the Hamiltonian a number, λ , is assigned to the eigenvalues,

with $\lambda = 1$ for the lowest, etc. The pseudoquantum number λ always uniquely distinguishes the eigenvalues in a subblock F, since states with the same symmetry may not cross.

Many of the matrix element calculations were programmed by Hodgeson¹⁶. Programs to compute 6j and 9j symbols were written by Mr. E. E. Sibert. A spectrum plotting routine was written by Mr. Neal Rachlin. The line intensities are plotted against frequency to provide a useful means of comparing observed and calculated spectra.

EXPERIMENTAL

A 50 cc-atm sample of oxygen containing 55.45%¹⁷O was obtained from Yeda Research and Development Co., Rheovoth, Israel. ¹⁴N¹⁶O¹⁷O is prepared by the reaction



The reaction is rapid and complete. The equilibrium



is present. Spectral measurements were made at dry-ice temperature, where the equilibrium strongly favors N₂O₄. It was necessary to renew the sample at about five minute intervals because of chemical reaction with the waveguide.

A conventional 100 kc/sec Stark-modulated spectrometer was used. The klystron was mechanically driven at approximately 7 Mc/sec/min. The output of the phase

sensitive detector was displayed on a strip chart recorder. Frequency measurements were made by calibrating the fundamental of a Gertsch model FM-4 microwave frequency multiplier with a Hewlett-Packard model 5253A 100-500 Mc/sec frequency counter, and beating the output of the Gertsch with the klystron radiation. The beat note was detected on a 0-35 Mc/sec radio receiver. Markers corresponding to the beat note were spaced at approximately 2 Mc/sec intervals on the recorder tracing. Line frequencies were measured by linear interpolation between markers. Frequency measurements are believed accurate to ± 0.3 Mc/sec.

The signal to noise ratio of the strongest line is approximately 20 at the maximum sensitivity of the spectrometer. The spectrometer is not suitable for making reliable relative intensity measurements of widely spaced lines. However, the crude, strong line-weak line, intensity comparisons which could be made were very useful in seeking an initial assignment.

SPECTRUM AND INTERPRETATION

The rotational constants of $^{14}\text{N}^{16}\text{O}^{17}\text{O}$ were calculated by the use of Kraitchman's equations³³ from the rotational constants and r_s structure of $^{14}\text{N}^{16}\text{O}_2^{14}$. They are $A = 237617$, $B = 12608.87$ and $C = 11950.51$ Mc/sec. Using these rotational constants, the rigid rotor spectrum of

$^{14}\text{N}^{16}\text{O}^{17}\text{O}$ was predicted. The $8_{08} \rightarrow 7_{17}$ transition lies at 19.91 and the $9_{19} \rightarrow 10_{0,10}$ at 34.46 Kmc/sec. There is known to be a slight shift (≈ 20 Mc/sec) of both of these lines due to centrifugal distortion.

In the region 19.4-20.4 Kmc/sec some 130 lines have been observed and in the region 34.2-34.6 Kmc/sec some 60 lines have been observed. In general, the $8_{08} \rightarrow 7_{17}$ region appears to be a mass of very closely spaced lines, with only one prominent feature. A line stronger than any other by about a factor of two appears at 20153.6 Mc/sec. The $9_{19} \rightarrow 10_{0,10}$ region appears to have an approximate center of symmetry at about 34.46 Kmc/sec. This suggests that J scheme coupling is fairly pure for this transition, and that the two subbands correspond to N+S and N-S levels. The observed spectrum is plotted in Figure 2, and the assigned lines are given in Table VII.

The assignment of the lines was greatly simplified by the availability of the spin-rotation coupling constants for $^{14}\text{N}^{16}\text{O}_2$ and $^{14}\text{N}^{16}\text{O}^{18}\text{O}$, and the Fermi, dipole-dipole and quadrupole coupling constants for the ^{14}N nucleus¹⁴. Additionally, the quadrupole moment of the ^{17}O nucleus is known to be nearly zero³⁴, forcing the ^{17}O quadrupole coupling constants to be small. There are then only three parameters for which good initial estimates are not available. They are the Fermi and dipole-dipole coupling

constants of the ^{17}O nucleus.

An initial assignment of the $8_{08} \rightarrow 7_{17}$ transitions was made using the lines measured by Hodgeson¹⁶. The predicted $8_{08} \rightarrow 7_{17}$ spectrum is such that for nearly all reasonable values of the ^{17}O coupling constants, the $F\ 12 \rightarrow 11$, $\lambda 1 \rightarrow 1$ transition is stronger than any other line by a factor of ≈ 2 . The observed spectrum also has a similar line at about the same frequency. Hodgeson¹⁶ correctly assigned the $F\ 12 \rightarrow 11$, $\lambda 1 \rightarrow 1$ transition as the line he measured at 20154.1 Mc/sec. An analysis of the relative location of $F\ 10 \rightarrow 9$, $\lambda 1 \rightarrow 2$, $F\ 11 \rightarrow 10$, $\lambda 2 \rightarrow 3$ and $F\ 11 \rightarrow 10$, $\lambda 1 \rightarrow 2$ transitions with large changes in the ^{17}O coupling constants revealed that they were likely to be the lines measured by Hodgeson at 20113.2, 20181.8, and 20219.3 Mc/sec respectively. A least squares fit on the unknown ^{17}O parameters using these four lines yielded a spectrum which accounted for most of the lines observed by Hodgeson. With good starting values for all the hyperfine parameters available the assignment shown in Table VII was made.

The method used in refining the new ^{17}O coupling constants to best fit the observed spectrum is somewhat indirect. In spite of the fact that there are many more observations (≈ 150) than there are parameters to be determined (15), it is not possible to find a unique mathematical solution. The linear combination $\approx 2A_s - C_s$ is

essentially undetermined from our data and this is reflected as a large uncertainty in these parameters when a full least square analysis is performed.

In view of the fact that the subscript s parameters are known for $^{14}\text{N}^{16}\text{O}_2$ and $^{14}\text{N}^{16}\text{O}^{18}\text{O}$, a way to refine our data would be the usual least square technique³⁵, but with the subscript s parameters fixed. This method has certain disadvantages in that errors in the values taken for A_s , B_s , and C_s will cause errors in the determination of other hyperfine parameters. There was available to this author a diagnostic technique for determining the sources of poor convergence in a least square fit. The method is due to R. F. Curl³⁶. A brief description is given in Appendix IV.

TABLE VII

HYPERFINE ASSIGNMENT OF $^{14}\text{N}^{16}\text{O}^{17}\text{O}$			
$8_{08} \rightarrow 7_{17}$			
$F' \rightarrow F$	$\lambda' \rightarrow \lambda$	ν_{obs} (Mc/sec)	$\nu_{\text{calc}} - \nu_{\text{obs}}$ (Mc/sec)
12-11	1-1	20 153.6	+0.7
11-10	3-1	19 455.8	+0.1
	3-3	19 772.7	+0.3
	1-1	20 014.4	0.0
	2-2	20 069.9	+0.2
	2-3	20 181.9	+0.2
	1-2	20 219.1	+0.4
10-9	5-2	19 408.3	-0.1
	4-1	19 463.2	+0.4
	5-3	19 549.0	0.0
	4-3	19 666.2	0.0
	5-4	19 672.0	+0.1
	3-1	19 786.5	+0.3
	3-2	19 848.7	0.0
	4-5	19 853.4	0.0
	2-1	19 937.9	+0.2
	1-1	20 051.3	0.0
	1-2	20 112.9	+0.3
	3-4	20 112.9	-0.3

TABLE VII (continued)

HYPERFINE ASSIGNMENT OF $^{14}\text{N}^{16}\text{O}^{17}\text{O}$			
$8_{08} \rightarrow 7_{17}$			
$F' \rightarrow F$	$\lambda' \rightarrow \lambda$	ν_{obs} (Mc/sec)	$\nu_{\text{calc}} - \nu_{\text{obs}}$ (Mc/sec)
9-8	2-3	20 140.8	-0.2
	3-5	20 176.5	+0.2
	1-3	20 253.8	+0.1
	5-2	19 433.0	-0.2
	6-3	19 458.2	-0.3
	4-1	19 481.8	+0.3
	4-2	19 542.4	-0.1
	5-3	19 561.7	0.0
	6-4	19 596.3	-0.5
	6-5	19 649.0	0.0
	4-3	19 671.2	+0.1
	5-4	19 699.4	+0.2
	5-5	19 752.7	+0.1
	2-1	19 881.6	+0.2
	4-6	19 913.0	+0.2
	3-3	19 916.1	+0.1
	2-2	19 942.4	-0.4
	1-2	20 048.8	-0.1
	3-4	20 054.0	0.0
	3-5	20 107.3	0.0
	3-6	20 158.2	0.0

TABLE VII (continued)

HYPERFINE ASSIGNMENT OF $^{14}\text{N}^{16}\text{O}^{17}\text{O}$			
$8_{08}^{-7} 17$			
$F' \rightarrow F$	$\lambda' \rightarrow \lambda$	ν_{obs} (Mc/sec)	$\nu_{\text{calc}} - \nu_{\text{obs}}$ (Mc/sec)
	2 \rightarrow 4	20 208.8	0.0
	2 \rightarrow 6	20 312.8	+0.1
	1 \rightarrow 4	20 315.9	-0.3
8 \rightarrow 7	6 \rightarrow 3	19 492.5	+0.1
	4 \rightarrow 1	19 504.5	+0.3
	4 \rightarrow 2	19 563.8	0.0
	5 \rightarrow 3	19 589.1	+0.1
	4 \rightarrow 3	19 689.8	+0.1
	6 \rightarrow 5	19 715.2	+0.1
	5 \rightarrow 4	19 755.7	-0.3
	5 \rightarrow 5	19 811.5	+0.3
	2 \rightarrow 1	19 839.5	0.0
	4 \rightarrow 6	19 957.8	+0.2
	1 \rightarrow 2	19 997.3	+0.1
	2 \rightarrow 3	20 024.7	0.0
	3 \rightarrow 5	20 086.0	+0.1
	1 \rightarrow 3	20 123.6	0.0
	3 \rightarrow 6	20 131.5	0.0
	2 \rightarrow 4	20 191.0	0.0

TABLE VII (continued)

HYPERFINE ASSIGNMENT OF $^{14}\text{N}^{16}\text{O}^{17}\text{O}$			
$8_{08} \rightarrow 7_{17}$			
$F' \rightarrow F$	$\lambda' \rightarrow \lambda$	ν_{obs} (Mc/sec)	$\nu_{\text{calc}} - \nu_{\text{obs}}$ (Mc/sec)
7→6	4→2	19 586.0	0.0
	5→3	19 621.2	-0.2
	4→3	19 711.7	+0.1
	6→4	19 713.6	-0.2
	2→1	19 808.3	+0.5
	5→5	19 859.4	+0.1
	4→4	19 893.1	+0.1
	1→2	19 954.9	-0.2
	4→6	19 990.6	+0.2
	3→4	20 000.2	+0.2
	3→5	20 057.6	-0.2
	1→3	20 080.4	+0.1
	3→6	20 097.3	+0.6
	2→4	20 173.4	-0.3
	2→5	20 230.4	-0.2
	1→4	20 261.8	+0.1
	1→5	20 318.9	+0.1
6→5	5→3	19 573.3	-0.4
	3→2	19 612.7	-0.2
	4→3	19 655.3	-0.4

TABLE VII (continued)

HYPERFINE ASSIGNMENT OF $^{14}\text{N}^{16}\text{O}^{17}\text{O}$			
$8_{08}^{-7}17$			
$F' \rightarrow F$	$\lambda' \rightarrow \lambda$	ν_{obs} (Mc/sec)	$\nu_{\text{calc}} - \nu_{\text{obs}}$ (Mc/sec)
	3-3	19 739.2	-0.1
	2-1	19 788.6	+0.5
	5-5	19 818.9	+0.1
	2-2	19 842.9	0.0
	1-2	19 918.4	-0.3
	3-4	19 928.9	-0.7
	3-5	19 985.6	-0.3
	2-5	20 215.6	-0.1
	1-4	20 233.9	-0.3
5-4	3-2	19 615.0	-0.2
	2-2	19 693.0	-0.1
	3-3	19 807.5	-0.1
	1-1	19 885.5	-0.3
	1-3	20 205.8	-0.2

TABLE VII (continued)

HYPERFINE ASSIGNMENT OF $^{14}\text{N}^{16}\text{O}^{17}\text{O}$ $^9_{19}-^{10}_{0,10}$

$F' \rightarrow F$	$\lambda' \rightarrow \lambda$	ν_{obs} (Mc/sec)	$\nu_{\text{calc}} - \nu_{\text{obs}}$ (Mc/sec)
13→14	1→1	34 248.9	-0.1
12→13	1→1	34 277.2	+0.1
	2→2	34 292.1	+0.2
	3→3	34 599.2	-0.2
11→12	2→1	34 201.6	0.0
	1→1	34 256.9	+0.2
	2→2	34 316.2	0.0
	3→3	34 327.7	0.0
	1→2	34 371.5	+0.1
	4→4	34 562.7	-0.2
10→11	4→3	34 198.6	-0.2
	3→2	34 207.7	+0.1
	2→1	34 238.4	0.0
	1→1	34 298.3	+0.2
	2→2	34 348.9	+0.1
	3→3	34 356.0	+0.1
	1→2	34 408.8	+0.2
	5→4	34 469.9	+0.1

TABLE VII (continued)

HYPERFINE ASSIGNMENT OF $^{14}\text{N}^{16}\text{O}^{17}\text{O}$			
$9_{19-10}^{0,10}$			
$F' \rightarrow F$	$\lambda' \rightarrow \lambda$	ν_{obs} (Mc/sec)	$\nu_{\text{calc}} - \nu_{\text{obs}}$ (Mc/sec)
	4 \rightarrow 4	34 531.5	0.0
	6 \rightarrow 5	34 541.2	-0.4
	5 \rightarrow 5	34 583.2	0.0
9 \rightarrow 10	3 \rightarrow 2	34 225.0	0.0
	2 \rightarrow 1	34 269.6	+0.3
	1 \rightarrow 1	34 330.9	+0.2
	2 \rightarrow 2	34 375.5	+0.1
	3 \rightarrow 3	34 377.9	-0.2
	1 \rightarrow 2	34 436.6	+0.2
	5 \rightarrow 4	34 444.7	+0.2
	5 \rightarrow 5	34 552.8	+0.1
	6 \rightarrow 6	34 605.8	-0.1
8 \rightarrow 9	2 \rightarrow 1	34 297.3	0.0
	4 \rightarrow 3	34 300.7	+0.2
	1 \rightarrow 1	34 356.0	0.0
	3 \rightarrow 3	34 393.4	-0.2
	2 \rightarrow 2	34 397.2	-0.6
	5 \rightarrow 4	34 428.2	-0.1
	1 \rightarrow 2	34 455.8	0.0

TABLE VII (continued)

HYPERFINE ASSIGNMENT OF $^{14}\text{N}^{16}\text{O}^{17}\text{O}$			
$9_{19}^{-10}_{0,10}$			
$F' \rightarrow F$	$\lambda' \rightarrow \lambda$	ν_{obs} (Mc/sec)	$\nu_{\text{calc}} - \nu_{\text{obs}}$ (Mc/sec)
	6 \rightarrow 5	34 480.6	-0.1
	4 \rightarrow 4	34 483.4	0.0
	5 \rightarrow 5	34 530.5	0.0
	6 \rightarrow 6	34 575.2	0.0
	3 \rightarrow 4	34 576.2	-0.2
	4 \rightarrow 5	34 585.5	+0.3
7 \rightarrow 8	2 \rightarrow 1	34 322.6	-0.1
	1 \rightarrow 1	34 372.7	+0.3
	2 \rightarrow 2	34 414.6	+0.2
	4 \rightarrow 3	34 423.3	-0.1
	5 \rightarrow 4	34 465.2	-0.2
	3 \rightarrow 3	34 509.0	0.0
	4 \rightarrow 4	34 520.9	+0.1
	5 \rightarrow 5	34 554.8	0.0
	3 \rightarrow 4	34 606.9	-0.2
6 \rightarrow 7	1 \rightarrow 1	34 377.9	+0.5
	3 \rightarrow 2	34 461.2	+0.1
	2 \rightarrow 2	34 542.8	-0.3

TABLE VII (continued)

HYPERFINE ASSIGNMENT OF $^{14}\text{N}^{16}\text{O}^{17}\text{O}$			
$^9_{19-10}_{0,10}$			
$F' \rightarrow F$	$\lambda' \rightarrow \lambda$	ν_{obs} (Mc/sec)	$\nu_{\text{calc}} - \nu_{\text{obs}}$ (Mc/sec)
	3-3	34 547.5	0.0
5-6	1-1	34 566.3	-0.3

The diagnostic method is extremely helpful in the analysis of the data reported here. The eigenvector corresponding to the smallest eigenvalue of the system of normal equations associated with our data is concerned primarily with A_s and C_s , with B_s to a lesser extent, and to a very slight extent with the remainder of the hyperfine parameters.

We therefore have very good estimates of the subscript I and Q hyperfine parameters determined by our data without carrying out a full least squares analysis. The final parameters obtained are given in Table VIII, along with the most precise values of the ^{14}N coupling constants available from work on other isomers of nitrogen dioxide³⁷. The uncertainties quoted σ_{est} were obtained from the mean standard deviations (S) and the variances (B_{ii}^{-1}) in the parameters; $\sigma_{\text{est}} = S(B_{ii}^{-1})^{\frac{1}{2}}$.

The errors (calc-obs) in the assigned lines were obtained using the parameters in column two of Table VIII. Calculated frequencies were corrected by a constant term which accounts for centrifugal distortion and small errors in the rotational constants.

TABLE VIII

		Lees, <i>et al.</i> ^a	This Work	Combined ^d
		¹⁴ N ¹⁶ O ₂ Basis	¹⁴ N ¹⁶ O ¹⁷ O	¹⁴ N ¹⁶ O ₂ Basis
		(Weighted)		
A _s	^b	5401.74±0.07 $\frac{\text{Mc}}{\text{sec}}$		$\frac{\text{Mc}}{\text{sec}}$ 5401.74±0.07 $\frac{\text{Mc}}{\text{sec}}$
B _s	^b	7.65±0.02		7.65±0.02
C _s	^b	-95.24±0.07		-95.24±0.02
(0) _I (¹⁷ O)	^c		-63.76±0.03	-63.76±0.03
(aa) _I (¹⁷ O)	^c		50.48±0.08	50.48±0.08
(cc) _I (¹⁷ O)	^c		55.85±0.10	55.85±0.10
(0) _I (¹⁴ N)		147.27±0.03	147.28±0.05	147.27±0.03
(aa) _I (¹⁴ N)		-22.23±0.07	-21.93±0.14	-22.23±0.07
(cc) _I (¹⁴ N)		-17.60±0.08	-17.00±0.24	-17.60±0.08
(aa) _Q (¹⁷ O)	^c		-0.202±0.014	-0.202±0.014
(cc) _Q (¹⁷ O)	^c		-0.009±0.016	-0.009±0.016
(aa) _Q (¹⁴ N)		0.36±0.06	0.41±0.08	0.36±0.06
(cc) _Q (¹⁴ N)		1.30±0.05	1.33±0.15	1.30±0.05

^a Reference (37).

^b A_s, B_s, and C_s are poorly determined by our data. See text.

^c Not determined from previous work.

^d Spin-rotation and ¹⁴N coupling constants taken from Reference (37), ¹⁷O coupling constants from this work. No adjustment of ¹⁷O parameters was made to correct for the slight asymmetry of ¹⁴N¹⁶O¹⁷O.

DISCUSSION OF THE MAGNETIC COUPLING CONSTANTS

A complete interpretation of the hyperfine coupling constants in nitrogen dioxide must await more exact quantum mechanical calculations than are available at present. However, it is possible to make some comments about the general nature of the odd electron orbital in the vicinity of the oxygen nucleus.

The molecular symmetry of NO_2 corresponds to that of the C_{2v} point group. Hijikata, Lin, and Baird³⁸ have analyzed the data from microwave and electron spin resonance spectra of NO_2 and concluded that the odd electron orbital has the symmetry of the a_1 (fully symmetric) representation. Bird *et al.*¹⁴ have interpreted their values of $(0)_{\text{I}(^{14}\text{N})}$, $(aa)_{\text{I}(^{14}\text{N})}$ and $(cc)_{\text{I}(^{14}\text{N})}$ as indicating that the odd electron orbital has 9-10% 2s character and between 26 and 52% 2p character on the nitrogen atom, directed along the axis of symmetry.

The Fermi constant $(0)_{\text{I}(^{17}\text{O})}$ can be interpreted in terms of the 2s character of the odd electron on oxygen. To estimate the 2s character we need only the magnitude of $|\psi(0)|^2$ for an idealized 100% 2s oxygen electron. This may be obtained approximately from a Hartree-Fock 2s atomic oxygen orbital. This approach was also used by Miller, Townes, and Kotani³⁹ in interpreting the Fermi constant of $^{16}\text{O}^{17}\text{O}$. Their value of

$(0)_{I(17O)}$ is -56 Mc/sec and is comparable to our value of -63.76 Mc/sec. Both indicate that the odd electron has 2-3% 2s character on the oxygen atom.

To estimate the 2p character of the odd-electron orbital on oxygen, calculation of the oxygen dipole-dipole constants for an idealized 100% 2p oxygen orbital is needed. The value of $\left\langle \frac{1}{r^3} \right\rangle = 29 \times 10^{24} \text{ cm}^{-3}$,²⁶ based on a pure 2p in atomic oxygen, is used here. Our value of $(cc)_{I(17O)}$ indicates approximately 45% 2p character on oxygen.

In view of the extensive data now available on the hyperfine coupling constants in nitrogen dioxide, a LCAO-MO can be estimated for the odd electron. A 2s 2p approximation similar to that made by Fischer-Hjalmars⁴⁰ on O_3 is used. To facilitate comparison with her calculations we adopt the basis

$$\begin{aligned} \psi(4a_1) = & \frac{C_1}{\sqrt{2}}[2s(O_1) + 2s(O_2)] + C_2 2s(N) + \frac{C_3}{\sqrt{2}}[(2p_b(O_1) + 2p_b(O_2))] \\ & + C_4 2p_b(N) + \frac{C_5}{\sqrt{2}}[(2p_a(O_1) - 2p_a(O_2))], \end{aligned}$$

where a and b refer to the inertial axes of the molecule.

From the estimates discussed above, we obtain $C_1^2 = .06$, $C_2^2 = .09$, $C_3^2 = .88$, $C_4^2 = .45$ and $C_5^2 = .03$. For the $4a_1$ orbital of o zone, by a LCAO-SCF-MO calculation, Fischer-Hjalmars⁴⁰ obtains

$$C_1^2 = .0061; C_2^2 = .0275, C_3^2 = .920, C_4^2 = .218, \text{ and } C_5^2 = .054.$$

Curl⁴¹ has constructed a set of LCAO-MO orbitals assuming sp^2 hybridization and equivalence of 1-electron Coulomb integrals, and used them to discuss the hyperfine coupling constants in ClO_2 . The coefficients of his $4a_1$ orbital may be placed on our basis by assuming a bond angle of 120° . Then $C_1^2 = 0$, $C_2^2 = .17$, $C_3^2 = .38$, $C_4^2 = .33$, and $C_5^2 = .13$. This simplified orbital appears to give less good agreement with the observed coupling constants than does the orbital of Fischer-Hjalmar⁴⁰.

CHAPTER III
A MICROWAVE SPECTROMETER FOR
SIMPLE UNSTABLE MOLECULES

PURPOSE

Perhaps the most challenging area of chemical research today is the study of the chemical and physical properties of unstable, or reactive molecules. Short-lived species appear to play an important role as intermediates in many chemical reactions. Of the varied methods which are being used to study these molecules, microwave spectroscopy has certain advantages. Among these are high resolution and very accurate measurement of small energy differences. The fundamental information which can be obtained from rotational spectra are molecular structural parameters. Many reactive species have a net electron spin or net orbital angular momentum. The microwave spectra of these molecules can yield a wealth of information, similar to that described in Chapter II, about molecular electronic structure and chemical bonding. It appears that a microwave spectrometer especially suited for the study of unstable molecules would be a valuable research tool.

BASIC DESIGN REQUIREMENTS

The application of microwave spectroscopy to the study of unstable molecules is by no means an idea which has originated in our laboratory. It is difficult to estimate how much effort has been extended in searching for the rotational spectra of reactive molecules. A conservative estimate would be 50 man-years. The totality of relatively unstable molecules which have assigned microwave spectra comprises a lamentably short list. They are OH, SO, SH, S₂O, CS, AlF, SeH, TeH, CN, and SiF₂^{18,19,42-48}. And for many of these molecules, much has been left undone. A discussion of the specific methods used in the production and detection of the spectra of each of these molecules will not be presented here. There is ample description in the references cited. Spectrometer design appears to have been as varied as the molecules studied, and in every case much trial and error manipulation of the apparatus was necessary to produce the molecule in detectable concentrations. This is a result of a general uncertainty about the chemical properties (e.g., reaction mechanisms and rates) of reactive molecules. A conclusion to be drawn from the studies mentioned above is that the production and detection, by microwave methods, of unstable molecules requires a major effort, and the chances for success are usually not well established.

In the light of these facts, several features which

it would be desirable to include in the design and construction of a versatile microwave spectrometer for the study of unstable molecules may be outlined.

First, from the very nature of the problem, a fast flow system is indicated. Reactive molecules are not in equilibrium with their environment, and must be continuously generated and passed through the absorption cell. (An alternative procedure would be a rapid-scan microwave spectrometer and generate unstable molecules by high energy pulsation of stable molecules. Such an instrument is under construction at the University of California). Physically, in addition to a fast pumping device, a fast flow of low density gas requires that the absorption cell and exhaust system have a large cross-sectional area.

Secondly, it is generally true that reactive molecules tend to recombine at metal surfaces at a much higher rate than at a non-metallic surface, such as glass or teflon. Thus, it is desirable that the portion of the spectrometer from the inlet system through the absorption cell be devoid of metallic surfaces. This, and the above requirement of rapid flow, precludes the use of Stark modulation to improve the sensitivity of the spectrometer. The Stark field must be set up by electrodes in close proximity to the sample.

Thirdly, the loss in sensitivity in a video spectrometer

as opposed to a Stark-modulation spectrometer, can be partially regained by increasing the operating frequency. Since absorption intensity in the microwave region increases approximately as the square of frequency, operation at millimeter wavelengths can give 100 times the sensitivity of a video spectrometer operating in the conventional centimeter region. If the molecule of interest is a free radical, Zeeman modulation may be applied to further increase sensitivity. The magnetic field strength required is moderate and may be easily produced by an external solenoid. The necessity to operate at high frequencies is not a severe limitation in terms the type of rotational spectra which may be observed. In general, the transitions of primary interest are the low J transitions. For simple molecules with small moments of inertia these transitions are usually in the millimeter region.

Lastly, in view of the existing uncertainty in the optimum methods of producing unstable molecules, a versatile molecule generating system should be constructed so that various molecular dissociation processes and chemical reaction may be tried. Flowing a stable molecule through a microwave resonant cavity, or a high temperature zone are generally reliable ways of dissociating stable species into reactive intermediates. Excited molecules may also be reacted *in situ* with suitable cold molecules to produce

unstable species.

A spectrometer having the general features described above has been constructed. It is now being tested.

FUNDAMENTALS OF CONSTRUCTION

The basic design of our spectrometer is not original. A similar apparatus has been used by Kewley *et al.*^{44(b)} to obtain the spectra of CS and SO. Improvements on their system have been suggested by Dr. K. V. L. N. Sastry⁴⁹.

Methods of achieving a fast flow vacuum system are well known and the details will not be reported here. We believe molecules with half lives on the order of milliseconds can be detected in our spectrometer.

Because of the requirements of rapid throughput from the molecule source to the exhaust system, and the necessity to eliminate metal-sample reactions, our absorption cell is a 4" diameter glass tube, with teflon windows to permit the passage of the microwave beam. Overall length of the absorption cell is approximately 24". This may readily be varied if desirable.

The inlet for reactive species is directly into the absorption cell with minimal constrictions. We have readily available a 125 watt microwave generator and resonant cavity, high temperature furnaces, and an induction heater. All are easily connected to the inlet

flow system for production of reactive species by molecular dissociation processes. Secondary reactants may be introduced at several points.

The requirement of high frequency operation presents some special problems in radiation sources and microwave hardware which are not encountered in the conventional microwave region.

The teflon windows on the absorption cell are actually converging lenses. High-frequency radiation from a source whose dimensions are on the order of millimeters is brought up to the dimensions of the absorption cell by an S-band horn antenna, collimated by the first lens, passed through the absorption cell, and then refocussed by the second lens and passed through an S-band receiving horn to the detector.

Initial attempts at obtaining reliable mm-wave sources were concerned with the harmonic generation technique introduced by King and Gordy. This method consists essentially of inserting a non-linear crystal rectifier into a low frequency microwave beam and taking the harmonic output as a source of high-frequency radiation. Since the dimensions of the rectifying element must be small in comparison to the radiation wavelength, the construction and manipulation of the harmonic generator are exacting. The rectifier contact is formed by electrolytically sharpening a fine tungsten wire

($\approx .002$ " diameter) and lightly touching the wire to the surface of small chip of a semiconductor, such as boron-doped silicon. Detection of the high frequency radiation is similar in principle, but the detector is somewhat simpler in construction because of the absence of the fundamental frequency.

The excellent results obtained by Gordy and co-workers^{19,50,51} using this technique on both stable and unstable molecules are well known. However, we have found the harmonic generation technique to be extremely tedious at best. The chief problems are difficulty in identifying the principal harmonic number of the radiation from a particular rectifier contact, and a general instability of the point contacts, especially at the detector.

Recently we have obtained a klystron which oscillates in the 95-105 Kmc/sec region. It can conservatively be estimated that one day of searching with this klystron is equivalent to weeks of work using the harmonic generation technique. While harmonic generation is in principal very versatile in terms of range of output frequency, for the reasons cited above, high-frequency klystrons seem to be the most economical sources for mm-wave spectroscopy.

In the brief period that the instrument described above has been operating usefully as a spectrometer, assigned transitions belonging to the stable molecules OCS and SO₂

have been readily observed. Initial attempts to observe the SO transition at 99299.9 Mc/sec¹⁹ by passing SO₂ through a microwave discharge have been unsuccessful. This is not surprising in light of the major effort which is usually involved in seeking the optimum conditions for production of a reactive molecule in any particular experimental arrangement. Initial failures are certainly not to be taken as conclusive in the attempt to find new reactive species.

PROSPECTIVE MOLECULES

The extensive compilation by Herzberg⁵² is a useful list of reactive diatomic molecules which are known to exist. However, the tabulated data were obtained by visible and ultraviolet spectroscopy. It is unfortunate that present microwave spectrometers do not approach the sensitivity obtainable in optical spectroscopy.

The recent work of Carrington and Levy⁵³ on the gas phase electron spin resonance spectra of ClO, BrO, and NS indicate that these molecules may have detectable microwave spectra. The ground electronic state of ClO is a $^2\Pi_{3/2}$ and the J 3/2-5/2 transition should lie at about 96.3 Kmc/sec (for ³⁵Cl)⁵⁴. ⁷⁹BrO has a similar electronic structure and the J 5/2-7/2 transition should occur at approximately 94.5 Kmc/sec⁵⁴. ¹⁴N³²S has a $^2\Pi_{1/2}$ ground state. The J 1/2-3/2 transition is at 70 Kmc/sec and the J 3/2-5/2 is at 166 Kmc/sec⁵⁵.

The molecule S_2 exists as the predominant species in low pressure sulfur vapor at about $500^\circ C$ ⁵⁶. It may be possible to obtain sufficient concentrations of S_2 by flowing sulfur vapor through a hot tube furnace. The transitions are magnetic dipole ($^3\Sigma$ ground state) as in oxygen. While the transitions are expected to be weaker than those in oxygen, they may be observable, since $^{16}O^{17}O$ was studied with a sample $\approx 1\%$ enriched in ^{17}O ⁵⁷.

There are many other species which may have detectable microwave spectra. While searching for these new species is difficult and uncertain, the new information which may be gained is of great value.

APPENDIX INucleus 2 Matrix Elements Diagonal in NT

$$\langle NTSJ' I_1 F_1 I_2 F | H_f(2) | NTSJ I_1 F_1 I_2 F \rangle$$

$$= (-1)^{N+S+2J'+I_1+2F_1+I_2+F} (0)_{I_2}.$$

$$1/4 [(2F_1+1)(2F_1'+1)(2J+1)(2J'+1)(2S)(2S+1)(2I_2)$$

$$(2I_2+1)(2I_2+2)]^{1/2}$$

$$\cdot \begin{Bmatrix} F_1' & F_1 & 1 \\ I_2 & I_2 & F \end{Bmatrix} \cdot \begin{Bmatrix} J' & J & 1 \\ F_1 & F_1' & I_1 \end{Bmatrix} \cdot \begin{Bmatrix} J' & J & 1 \\ S & S & N \end{Bmatrix}$$

$$\langle NTSJ' I_1 F_1 I_2 F | H_{dd}(2) | NTSJ I_1 F_1 I_2 F \rangle^a$$

$$= (-1)^{J'+I_1+2F_1+I_2+F} \sum_{I_2}$$

$$1/8 \left[\frac{30(2F_1+1)(2F_1'+1)(2J+1)(2J'+1)(2I_2)(2I_2+1)(2I_2+2)}{(2N-1)(2N+3)(2N+1)} \right. \\ \left. \times (2S)(2S+1)(2S+2)(2N)(2N+2) \right]^{1/2}$$

$$\cdot \begin{Bmatrix} F_1' & F_1 & 1 \\ I_2 & I_2 & F \end{Bmatrix} \cdot \begin{Bmatrix} J & J' & 1 \\ F_1 & F_1' & I_1 \end{Bmatrix} \cdot \begin{Bmatrix} N & N & 2 \\ J' & J & 1 \end{Bmatrix}$$

$$\begin{aligned}
& \langle NTSJ' I_1 F_1 I_2 F | H_q(2) | NTSJI_1 F_1 I_2 F \rangle \\
& = (-1)^{N+S+J+J'+I_1+2F_1+I+F} \sum Q_2 \\
& \quad 1/4 \left[\frac{(2F_1+1)(2F_1'+1)(2J+1)(2J'+1)(2I_2+1)(2I_2+2)(2I_2+3)}{(2N-1)(2N+3)(2N+1)} \right. \\
& \quad \quad \left. \times (2I_2)(2I_2-1)(2N)(2N+2) \right]^{\frac{1}{2}} \\
& \quad \cdot \left\{ \begin{matrix} N & N & 2 \\ J' & J & S \end{matrix} \right\} \cdot \left\{ \begin{matrix} J & J' & 2 \\ F_1 & F_1 & I_1 \end{matrix} \right\} \cdot \left\{ \begin{matrix} F_1' & F_1 & 2 \\ I_2 & I_2 & F \end{matrix} \right\}
\end{aligned}$$

-
- ² The \sum 's are defined in Appendix I, reference (23). They are functions of the coupling constants, N, and the rotational constants of the molecule.

H_{sr} and $H_{dd}(1)$ Matrix Elements Off-Diagonal in $N\tau$

$$\begin{aligned} & \langle N+1K_{-1} \gamma' S J I_1 F_1 I_2 F | H_{sr} | NK_{-1} \gamma S J I_1 F_1 I_2 F \rangle^a \\ &= \frac{-3K[(N+1)^2 - K^2]^{\frac{1}{2}} \{ (aa)_s + (-1)^{\frac{N\delta 1K}{6}} (N+1)(2(cc)_s + (aa)_s) \}}{4(N+1)} \end{aligned}$$

$$\begin{aligned} & \langle N+1K_{-1} \gamma' S J_+ I_1 F_1 I_2 F | H_{dd}(1) | NK_{-1} \gamma S J_+ I_1 F_1 I_2 F \rangle^a \\ &= [J(J-1) + I_1(I_1+1) - F(F+1)] 3K[(N+1)^2 - K^2]^{\frac{1}{2}} \\ & \quad \frac{\{ (aa)_{I_1} + (-1)^{\frac{N\delta 1K}{6}} (N+1)(2(cc)_{I_1} + (aa)_{I_1}) \}}{2(2N+1)(2N+3)(N+1)} \end{aligned}$$

$$\begin{aligned} & \langle N+1K_{-1} \gamma' S J_+ I_1 F_1 I_2 F | H_{dd}(1) | NK_{-1} \gamma S J_- I_1 F_1 I_2 F \rangle \\ &= (-1)^{J_- + I_1 + F_1} 9[(N+1)^2 - K^2]^{\frac{1}{2}} K \{ (aa)_{I_1} + (-1)^{\frac{N\delta 1K}{6}} (N+1)(2(cc)_{I_1} + (aa)_{I_1}) \} \\ & \quad \cdot \left[\frac{5I_1(I_1+1)(2I_1+1)(2J_-+1)}{6(N+2)(N)} \right]^{\frac{1}{2}} \end{aligned}$$

$$\cdot \begin{Bmatrix} J_- & J_+ & 1 \\ I_1 & I_1 & F_1 \end{Bmatrix} \cdot \begin{Bmatrix} N+1 & N & 2 \\ S & S & 1 \\ J_+ & J_- & 1 \end{Bmatrix}$$

$$\langle N-1K_{-1} \gamma' S J_{-1} F_1 I_2 F | H_{dd}(1) | NK_{-1} \gamma S J_{+1} F_1 I_2 F \rangle$$

$$= (-1)^{J_{+1} + I_1 + F_1} 9 [N^2 - K^2]^{\frac{1}{2}} K \{ (aa)_{I_1} (-1)^{N-1} \frac{\delta_{1K}}{6} N (2(cc)_{I_1} + (aa)_{I_1}) \}$$

$$\left[\frac{5I_1(I_1+1)(2I_1+2)(2J_{+1}+1)}{6(n-1)(n+1)} \right]^{\frac{1}{2}}$$

$$\cdot \begin{Bmatrix} J_{-} & J_{+} & 1 \\ I_1 & I_1 & F_1 \end{Bmatrix} \cdot \begin{Bmatrix} N-1 & N & 2 \\ S & S & 1 \\ J_{-} & J_{+} & 1 \end{Bmatrix}$$

^a See reference (22), Appendix.

APPENDIX III

64

Spectrum of $^{14}\text{N}^{16}\text{O}^{17}\text{O}$ Observed by Hodgeson

19 741.9 Mc/sec

19 801.1

19 853.7

19 860.2

19 881.9

19 885.7

19 901.6

19 913.4

19 918.5

19 938.2

19 960.5^a

20 014.4

20 113.2

20 154.1

20 181.8

20 219.3

20 266.8

^a Appeared as closely spaced doublet or triplet of lines.
The frequency given is that of the strongest member.

Diagnostic Least Squares

In the usual method of least squares on a nonlinear system³⁵, the equations of condition may be written as

$$Ax = a \quad (A1)$$

where A is the matrix of derivatives, x is a vector of parameter changes to be determined and a is the vector of initial differences between observation and calculation. Then

$$x = B^{-1}b, \quad (A2)$$

where $B = \tilde{A}A$ and $b = \tilde{A}a$. If one then iterates with $x^{(1)} = x^{(0)} + B^{-1}b$, $a^{(1)} = \text{obs} - \text{calc}^{(1)}$, and $A^{(1)}$, convergence of the system reduces the sum of the squares of the residuals to a minimum.

In the diagnostic method an orthogonal transformation O is found which diagonalizes B. Then

$$OB\tilde{O} = \lambda_i^* \quad (A3)$$

where the λ_i are the eigenvalues of B. Equation (A2) becomes

$$y_i = \frac{c_i}{\lambda_i} \quad (A4)$$

where $y = O x$ and $c = O b$. The y_i are eigenvectors of B

* λ_i should not be confused with the hyperfine energy level index λ .

and are orthogonol. It is then possible to carry out the least squares process in a stepwise fashion.

The smallest eigenvalue of B will be associated with the most poorly determined eigenvector. If the eigenvalues of B are arranged in decreasing order, then the parameter changes (σy_1) associated with the largest eigenvalue (λ_1) can be used to calculate c_2 (i.e., Ob), and the process repeated for λ_2 . It should be emphasized that the process is a full least squares if carried to completion, but if terminated because of the presence of a small eigenvalue λ_s no least squares fit is obtained. However, by knowing x_s (i.e., σy_s) some information has been gained about which particular linear combination of parameters is poorly determined by the data.

1. An excellent review of both theory and applications has been made by C. C. Lin and J. D. Swalen, *Rev. Mod. Phys.* 31, 841 (1959).
2. K. S. Pitzer, *Discussions Faraday Soc.* 10, 66 (1951).
3. D. R. Herschbach, *J. Chem. Phys.* 27, 975 (1957).
4. E. B. Wilson, Jr., *Proc. Natl. Acad. Sci. U. S.* 44, 211 (1958).
5. R. B. Kilb, C. C. Lin, and E. B. Wilson, Jr., *J. Chem. Phys.* 26, 1695 (1957).
6. M. T. Rogers, *J. Am. Chem. Soc.* 69, 2545 (1947).
7. D. R. Lide, Jr., *J. Chem. Phys.* 37, 2074 (1962).
8. D. R. Lide, Jr. and M. Jen, *Chem. Phys.* 40, 252 (1964).
9. K. B. McAfee, Jr., *Phys. Rev.* 78, 340(A) (1950); 82, 971(L) (1951).
10. G. R. Bird, *Phys. Rev.* 98, 1160 (1955).
11. G. R. Bird, *J. Chem. Phys.* 25, 1040 (1950).
12. J. Rosenthal, *Bull. Am. Phys. Soc.* 3, 214 (1958).
13. J. C. Baird and G. R. Bird, *Bull. Am. Phys. Soc.* 4, 68 (1959).
14. G. R. Bird *et al.*, *J. Chem. Phys.* 40, 3378 (1964).
15. J. C. Baird, Thesis, Rice Institute, 1959 (unpublished).
16. J. A. Hodgeson, Thesis, Rice University, 1965 (unpublished).
17. J. A. Hodgeson, E. E. Sibert, and R. F. Curl, Jr., *J. Phys. Chem.* 67, 2833 (1963).
18. G. C. Dousmanis, T. M. Sanders, Jr., and C. H. Townes, *Phys. Rev.* 100, 1735 (1955).
19. (a) F. X. Powell and D. R. Lide, Jr., *J. Chem. Phys.* 41, 1413 (1964); (b) M. Winnewisser, K. V. L. N. Sastry, and W. Gordy, *J. Chem. Phys.* 41, 1687 (1964).

20. (a) J. H. Burkhalter, R. S. Anderson, W. V. Smith, and W. Gordy, Phys. Rev. 79, 651 (1950); 77, 152(L) (1950); 79, 224(A) (1950); (b) M. Mizushima and R. M. Hill, Phys. Rev. 93, 745 (1954).
21. (a) C. A. Burrus and W. Gordy, Phys. Rev. 92, 1437 (1953); (b) J. J. Gallagher, F. D. Bedard, and C. M. Johnson, Phys. Rev. 93, 729 (1954).
22. (a) R. F. Curl, Jr., *et al.*, Phys. Rev. 121, 1119 (1961); (b) R. F. Curl, Jr., R. F. Heidelberg, and J. L. Kinsey, Phys. Rev. 125, 1993 (1962); (c) J. L. Kinsey, Thesis, Rice Institute, 1959 (unpublished).
23. R. F. Curl, Jr., and J. L. Kinsey, J. Chem. Phys. 35, 1758 (1961).
24. C. C. Lin, Phys. Rev. 116, 903 (1959).
25. J. G. Baker, Thesis, Cambridge, 1958 (unpublished).
26. C. H. Townes and A. L. Shawlow, "Microwave Spectroscopy", McGraw-Hill Book Co., Inc., New York, N. Y., 1955.
27. J. H. Van Vleck, Rev. Mod. Phys. 23, 213 (1951).
28. E. C. Kemble, "The Fundamental Principles of Quantum Mechanics", McGraw-Hill Book Co., Inc., New York, N. Y. 1937, p. 394.
29. G. Racah, Phys. Rev. 61, 186 (1942); 62, 438 (1942); 63, 307 (1943).
30. E. P. Wigner, "On Matricies Which Reduce Kronecker Products of Representations of Simply Reducible Groups", 1951 (unpublished).
31. A. R. Edmonds, "Angular Momentum in Quantum Mechanics", Princeton University Press, Princeton, N. J., 1957.
32. S. C. Wang, Phys. Rev. 34, 243 (1929).
33. J. Kraitichman, Am. J. Phys. 21, 17 (1953).
34. W. Gordy, W. V. Smith, and R. F. Trambarulo, "Microwave Spectroscopy", John Wiley and Sons, New York, N.Y., 1953.
35. See, for example, E. T. Whittaker and G. Robinson, "The Calculus of Observations", Blackie and Son, Ltd., London, 1924, Chapter IX.

36. R. F. Curl, Jr., private communication.
37. R. M. Lees, R. F. Curl, Jr., and J. G. Baker, to be published.
38. K. Hijikata, C. C. Lin, and J. C. Baird, J. Chem. Phys. 36, 1183 (1962).
39. S. L. Miller, C. H. Townes, and M. Kotani, Phys. Rev. 90, 542 (1953).
40. I. Fischer-Hjalmars, Arkiv För Fysik. 11, 529 (1957).
41. R. F. Curl, Jr., J. Chem. Phys. 37, 779 (1962).
42. H. E. Radford and M. Linzer, Phys. Rev. Let. 10, 443 (1963).
43. D. J. Meschi and R. J. Myers, J. Mol. Spect. 3, 405 (1959).
44. (a) R. C. Mockler and G. R. Bird, Phys. Rev. 98, 1837 (1955); (b) R. Kewley, K. V. L. N. Sastry, M. Winnewisser, and W. Gordy, J. Chem. Phys. 39, 2856 (1963).
45. D. R. Lide, J. Chem. Phys. 38, 2027 (1963).
46. H. E. Radford, J. Chem. Phys. 40, 2732 (1964).
47. K. M. Evenson, J. L. Dunn, and H. P. Broida, Phys. Rev. Let. 13, A3 (1964).
48. V. M. Rao, R. F. Curl, Jr., P. L. Timms, and J. L. Margrave, J. Chem. Phys. 43, 2557 (1965).
49. K. V. L. N. Sastry, private communication.
50. W. C. King and W. Gordy, Phys. Rev. 93, 407 (1954).
51. (a) O. R. Gilliam, C. M. Johnson, and W. Gordy, Phys. Rev. 78, 140 (1950); (b) C. A. Burrus, Jr., and W. Gordy, *ibid.* 92, 274 (1953); (c) 101, 599 (1956); (d) M. Cowan and W. Gordy, *ibid.* 111, 209 (1958); (e) P. G. Favero, A. M. Mirri, and W. Gordy, *ibid.* 114, 1534 (1959); (f) G. Jones and W. Gordy, *ibid.* 135, A295 (1964); (g) S. E. Veasy and W. Gordy, *ibid.* 138, A1303 (1965).
52. G. M. Herzberg, "Spectra of Diatomic Molecules", D. Van Nostrand Co. Inc., New York, N. Y., 1950.

53. A. Carrington, and D. H. Levy, 44 1928 (1966).
54. Based on the rotational constants obtained from fine structure of electronic transitions by R. A. Durie, and D. A. Ramsay, Can. J. Phys. 36, 35 (1958).
55. Rotational constant taken from the table of J. Smith, and B. Meyer, J. Mol. Spect. 14, 160 (1964).
56. F. D. Rice, "Free Radicals in Organic Chemistry", Advances in Chemistry Series No. 36, American Chemical Society, 1962.
57. S. L. Miller, and C. H. Townes, Phys. Rev. 90, 537 (1953).